Spatiotemporal regulations of Wee1 at the G2/M transition

Hirohisa Masuda[a], Chii Shyang Fong[a,*], Chizuru Ohtsuki[b], Tokuko Haraguchi[b,c,d], and Yasushi Hiraoka[b,c,d]

[a]Laboratory of Cell Regulation, Cancer Research UK, London Research Institute, Lincoln's Inn Fields Laboratories, London WC2A 3LY, United Kingdom; [b]Kobe Advanced ICT Research Center, National Institute of Information and Communications Technology, Kobe 651-2492, Japan; [c]Graduate School of Science, Osaka University, Toyonaka 560-0043, Japan; [d]Graduate School of Frontier Biosciences, Osaka University, Suita 565-0871, Japan

ABSTRACT **Wee1 is a protein kinase that negatively regulates mitotic entry in G2 phase by suppressing cyclin B–Cdc2 activity, but its spatiotemporal regulations remain to be elucidated. We observe the dynamic behavior of Wee1 in *Schizosaccharomyces pombe* cells and manipulate its localization and kinase activity to study its function. At late G2, nuclear Wee1 efficiently suppresses cyclin B–Cdc2 around the spindle pole body (SPB). During the G2/M transition when cyclin B–Cdc2 is highly enriched at the SPB, Wee1 temporally accumulates at the nuclear face of the SPB in a cyclin B–Cdc2-dependent manner and locally suppresses both cyclin B–Cdc2 activity and spindle assembly to counteract a Polo kinase–dependent positive feedback loop. Then Wee1 disappears from the SPB during spindle assembly. We propose that regulation of Wee1 localization around the SPB during the G2/M transition is important for proper mitotic entry and progression.**

Monitoring Editor
Fred Chang
Columbia University

Received: Jul 28, 2010
Revised: Dec 7, 2010
Accepted: Jan 3, 2011

INTRODUCTION

Cell cycle progression is regulated by the cycling actions of the cyclin–CDK complexes and positive and negative regulator proteins. Wee1 is a protein kinase that acts as a negative regulator of the cyclin B–Cdc2 (Cdk1) complex in G2 phase through phosphorylation of Tyr-15 on Cdc2 kinase. It also counteracts Cdc25 protein phosphatase, which acts as a positive regulator of the complex through dephosphorylation of the tyrosine residue (Nurse, 1990). In many organisms, the cyclin B–Cdc2 complex and the mitotic regulators including Wee1 have distinct subcellular localizations that alter according to the phase of the cell cycle. It remains to be determined how the activity and localization of Wee1 and other proteins are dynamically coordinated in the cell to regulate mitotic entry and progression.

In mammalian cells, cyclin B–Cdk1 constantly shuttles between the nucleus and the cytoplasm, and its steady-state localization seems to be determined by the relative rates of nuclear import and export (Hagting *et al.*, 1998; Toyoshima *et al.*, 1998; Yang *et al.*, 1998). Cyclin B–Cdk1 localizes mostly in the cytoplasm in the G2 phase of the cell cycle and also at the centrosome at late G2 phase. The cytoplasmic localization of the complex is due to the rapid nuclear export mediated by a nuclear export sequence (NES) in cyclin B (Hagting *et al.*, 1998; Toyoshima *et al.*, 1998; Yang *et al.*, 1998). In prophase, cyclin B–Cdk1 is rapidly imported into the nucleus, and this event triggers subsequent mitotic events (Heald *et al.*, 1993; Jin *et al.*, 1998). The phosphorylated mitotic form of cyclin B is first localized at the centrosome in prophase before being transported into the nucleus, suggesting that the centrosome may function as sites of integration for proteins that trigger mitosis (Jackman *et al.*, 2003). Cyclin B–Cdk1 shows progressive activation from prophase to prometaphase, and different thresholds of the activity seem to trigger specific mitotic events (Lindqvist *et al.*, 2007; Gavet and Pines, 2010), suggesting that spatial and temporal regulation of the cyclin B–Cdk1 activity is important for proper entry and progression of mitosis.

This article was published online ahead of print in MBoC in Press (http://www.molbiolcell.org/cgi/doi/10.1091/mbc.E10-07-0644) on January 13, 2011.

*Present address: Cell Biology Program, Memorial Sloan-Kettering Cancer Center, New York, NY 10065.

Address correspondence to: Hirohisa Masuda (hiro.masuda@cancer.org.uk).

Abbreviations used: BAF, barrier-to-autointegration factor; CD, chromodomain; EMM2, Edinburgh minimal medium 2; GFP, green fluorescent protein; 3HA, three tandem repeats of the influenza virus hemagglutinin epitope; mRFP, monomeric red fluorescent protein; NES, nuclear export sequence; NLS, nuclear localization sequence; 1-NM-PP1, 4-amino-1-(*tert*-butyl)-3-(1′-naphthylmethyl)pyrazolo[3,4-*d*]pyrimidine; PMSF, phenylmethylsulfonyl fluoride; SPB, spindle pole body; ts, temperature sensitive; YES, yeast extract and supplements.

Spatial and temporal regulation of the cyclin B–Cdk1 regulators, Cdc25 and Wee1, also seems to be required for proper entry into mitosis in mammalian cells. There are three isoforms of Cdc25, and each of them seems to have distinct localization patterns and roles in activation of cyclin B–Cdk1 (Lindqvist *et al.*, 2005). For instance, Cdc25C shuttles between the nucleus and the cytoplasm (Dalal *et al.*, 1999; Kumagai and Dunphy, 1999), is localized in the cytoplasm during interphase, and moves to the nucleus during prophase (Heald *et al.*, 1993), as is found in cyclin B–Cdk1. On the other hand, Wee1 is found almost exclusively in the nucleus during interphase (McGowan and Russell, 1995) and moves to the cytoplasm during prophase (Baldin and Ducommun, 1995), although the timing of its export relative to the timing of cyclin B–Cdk1 import has not been studied. In mammalian oocytes, keeping embryonic Wee1 (Wee1B) in the nucleus is important to maintain meiotic arrest, and its timely export to the cytoplasm is required for meiosis to resume (Oh *et al.*, 2010). These observations suggest that physical separation of cyclin B–Cdk1 from its inhibitor Wee1 is crucial for both mitotic and meiotic progression. It is unclear, however, how cyclin B–Cdk1 activation in the cytoplasm and the nucleus is regulated and coordinated by Cdc25 and Wee1 during the G2/M transition.

The centrosome is required for several regulatory functions including cell cycle transitions, stress response, and signal transduction (reviewed in Doxsey *et al.*, 2005). In the fission yeast *Schizosaccharomyces pombe*, the spindle pole body (SPB), the centrosome equivalent, is important for regulatory functions including mitotic entry (Petersen and Hagan, 2005; Fong *et al.*, 2009; Tallada *et al.*, 2009) and septation initiation network signaling (reviewed in Krapp and Simanis, 2008). Cyclin B–Cdc2 and its regulators are shown to localize at the SPB. *S. pombe* B-type cyclin Cdc13 localizes predominantly in the nucleus and to the SPB in late G2 (Yanagida *et al.*, 1999; Decottignies *et al.*, 2001). On the other hand, Cdc2 kinase localizes in the nucleus, at the SPB, and in the cytoplasm (Alfa *et al.*, 1990), and the nuclear localization of Cdc2 seems to be dependent on Cdc13 (Decottignies *et al.*, 2001). These observations suggest that most of the Cdc13–Cdc2 complex is localized in the nucleus and to the SPB at late G2 phase. Part of Cdc13–Cdc2 moves on the spindle at early M phase and leaves from the spindle in anaphase (Alfa *et al.*, 1990; Yanagida *et al.*, 1999; Decottignies *et al.*, 2001). Cdc25 is localized in both the cytoplasm and the nucleus in G2 phase, but with some enrichment in the nucleus. This nuclear Cdc25 increases up to late G2 phase and then decreases during anaphase (Lopez-Girona *et al.*, 1999). Although Cdc25 does not seem to be specifically localized to the SPB, it is linked to the SPB through the action of an SPB component, Cut12, and Polo kinase, Plo1. Indeed, dominant *cut12* mutations suppress the phenotype of *cdc25* mutant cells by boosting Plo1 activity at the SPB to compensate the reduction of Cdc25 activity (MacIver *et al.*, 2003; Hagan, 2008). Moreover, Plo1 recruitment to the SPB during the G2/M transition is required for a positive feedback control of Cdc13–Cdc2 activity and regulated/influenced by the SPB components Cut12 and Pcp1 (Hagan, 2008; Fong *et al.*, 2009). These observations suggest that the SPB is a major site for regulating mitotic entry.

Localization of Wee1 in wild-type *S. pombe* cells has not been extensively studied due to the low expression levels of Wee1. Previous studies of Wee1 localization in cells overproducing Wee1 have shown that Wee1 is localized in the nucleus, to the SPB, and to the medial cortical nodes (Wu *et al.*, 1996; Ding *et al.*, 2000; Matsuyama *et al.*, 2006; Moseley *et al.*, 2009). Wee1 is proposed to be inactivated at the cortical nodes by Wee1 inhibitors Cdr1–Cdr2, the activities of which are regulated by gradients of Pom1, a negative regulator of Cdr1–Cdr2, from cell ends (Martin and Berthelot-Grosjean, 2009; Moseley *et al.*, 2009). However, *pom1*Δ cells divide at the cell length shorter by 10–20% compared with wild-type cells, whereas *wee1-ts* cells divide by 50% shorter. These observations suggest that there may be a mechanism regulating Wee1 activity other than the Pom1–Cdr2–Cdr1 signaling pathway. Considering in vitro studies that show that Wee1 can phosphorylate Cdc2 only when Cdc2 forms a complex with cyclin B (Parker *et al.*, 1992), Wee1 may phosphorylate Cdc2 mostly in the nucleus and at the SPB, where the Cdc13–Cdc2 complex is predominantly localized. Therefore the control of Wee1 localization seems to be important for regulation of the Cdc13–Cdc2 complex activity. It remains to be determined how localization of Wee1 is spatially and temporally regulated around the G2/M transition and how it affects Cdc13–Cdc2 activity and mitotic entry and progression.

We report the dynamic behavior of *S. pombe* Wee1 at the G2/M transition. We present data showing a link between the ability of Wee1 to accumulate at the nuclear face of the SPB and the ability of Wee1 to negatively regulate Cdc13–Cdc2 activity and spindle assembly during the G2/M transition.

RESULTS

Wee1 is temporally enriched at the SPB during the G2/M transition

We studied the dynamic changes of the subcellular localization of Wee1 around the G2/M transition by live cell imaging using Wee1 tagged with N-terminal green fluorescent protein (GFP). We replaced wild-type *wee1*$^+$ with *GFP–wee1*, the expression of which was under the control of the endogenous promoter. To observe mitotic progression of the GFP–Wee1 cells, the SPB was labeled using Sid4–monomeric red fluorescent protein (mRFP), or microtubules were labeled using mCherry–Atb2. We found that GFP–Wee1 was localized mostly in the nucleus at mid-late G2 phase, was enriched at the SPB at 2–3 min before SPB separation, and had disappeared from the SPB after SPB separation (Figure 1, A and B). Nuclear Wee1 lasted through M phase but then gradually decreased during M phase, ultimately disappearing in late anaphase. In most cells, the SPB localization of Wee1 was limited to a short period around the G2/M transition as described above; however, in some cells, it was also observed at late G2 phase at lower and fluctuating levels (Figure 1, C and D). In these cells, Wee1 decreased at the SPB to the minimum levels ~1–2 min before its levels sharply increased before SPB separation (Figure 1E), suggesting that the removal of Wee1 from the SPB is strictly regulated at this point.

We also found that Wee1 started to accumulate at the SPB after the interphase arrays of cytoplasmic microtubules started to disassemble at 3–4 min before spindle formation and disappeared after a bipolar spindle formed (Figure 2A). To confirm that Wee1 accumulated at the SPB during the G2/M transition but not in the late G2 phase, the timing of Wee1 accumulation was compared with the timing when the mitotic proteins Plo1, Cut7, and Msd1 were enriched at the SPBs (Figure 2B). Polo-like kinase Plo1 is a marker of mitotic entry, and a major accumulation of Plo1 at the SPB is observed after Cdc2 kinase activation (Mulvihill *et al.*, 1999). Cut7 belongs to a family of kinesin-5, which is required for bipolar spindle assembly. Cut7 localizes in the nucleus during interphase and accumulates at the SPB and on spindles during mitosis (Hagan and Yanagida, 1992). Msd1 is involved in anchoring spindle microtubules to the SPB and localizes to the SPB in early M phase (Toya *et al.*, 2007). We observed that, in comparison to these proteins, Wee1 accumulation at the SPB was preceded by the recruitment of Plo1 to the SPB, almost concomitant with Cut7, and was consequently followed by Msd1 (Figure 2B). In addition, we also

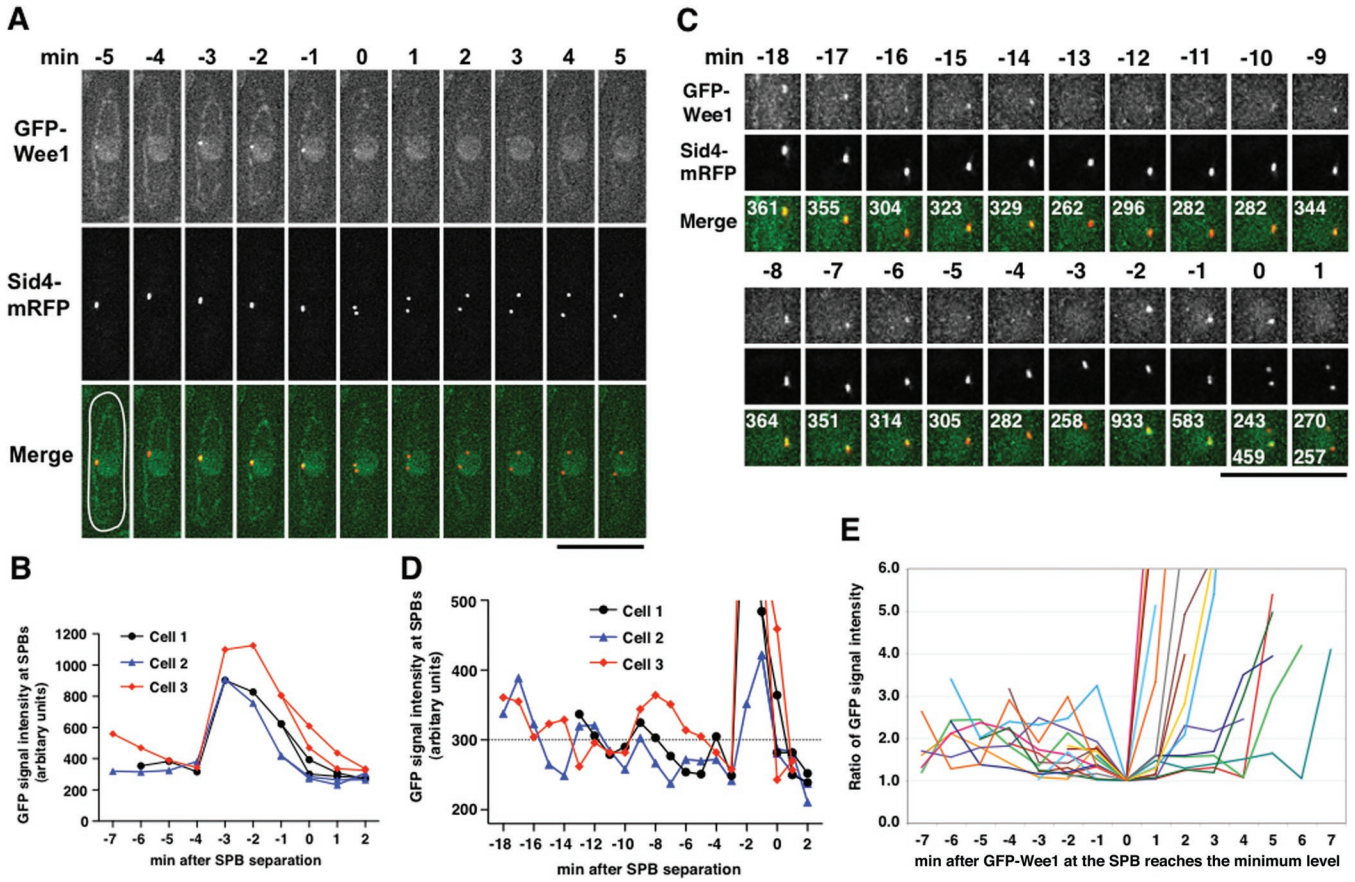

FIGURE 1: Wee1 dynamically localizes to the SPB. (A) GFP–Wee1 localizes in the nucleus and temporally accumulates at the SPB before SPB separation. Live images of a cell expressing GFP–Wee1 and Sid4–mRFP are shown at 1-min intervals. Time 0 represents when the two SPBs are separated for spindle assembly. GFP–Wee1 signal is observed in the nucleus and at the SPB. The fibrous structures observed in the cytoplasm are likely to come from the autofluorescence of mitochondrial flavoproteins (Kunz *et al.*, 1997). The cell shape is outlined in white on a merged image. (B) Quantification of the maximal intensity of GFP–Wee1 observed at the SPB. Data from three cells are shown. Cell 3 represents data from the cell shown in (A). (C) Levels of Wee1 localized at the SPB fluctuate during late G2. Live images of the SPB region of a cell expressing GFP–Wee1 and Sid4–mRFP. Images at 18 min before SPB separation through 1 min after SPB separation are shown. Maximal GFP signal intensity measured at the SPB is labeled at each time point on the merged image. (D) Quantification of GFP–Wee1 at the SPB in cells showing a fluctuation of Wee1 levels in late G2. Data from three cells are shown. Cell 3 represents the data from the cell shown in (C). (E) Wee1 localized at the SPB decreases to the minimum level before Wee1 is highly enriched at the SPB. Time 0 represents when the GFP signal intensity at the SPB reaches the minimum level. The ratio of GFP signal intensity to the minimum—$(I_t - I_{bg})/(I_0 - I_{bg})$, where I_{bg} is the background GFP intensity—is plotted at each time point until the signal intensity reaches the maximum level. Note that in 5, 6, and 1 out of the 16 cells observed, Wee1 levels at the SPB sharply increase at 1, 2, and 4 min after it reaches the minimum, respectively. In the other four cells, the GFP signal intensity at the SPB decreases to the minimum and then goes up and down once before it sharply increases. Bars, 10 μm.

examined the timing of accumulation of the B-type cyclin Cdc13 at the SPB. Cdc13 localizes predominantly in the nucleus and at the SPB in the G2 phase of the cell cycle (Decottignies *et al.*, 2001). The accumulation of Cdc13 at the SPB started to increase sharply ~6 min before SPB separation, peaked at 3 min before separation, and decreased to the levels of late G2 after separation (Figure 2, C and D). The beginning of increase in the levels of Cdc13 accumulated at the SPB seemed to correspond to the start of the G2/M transition, due to always being followed by SPB separation. The levels of Wee1 at the SPB stayed low when Cdc13 was accumulating at the SPB and then temporally increased around the time when levels of Cdc13 at the SPB reached their peak (Figure 2D). Thus the peak of SPB accumulation of Cdc13 is followed by the accumulation of Wee1 at the SPB. On the basis of these observations, we define here that the G2/M transition starts when Cdc13 starts to increase in levels at the SPB (at ~6 min before SPB separation) and ends when a bipolar spindle forms (at the time of SPB separation) (Figure 2D). To study whether Cdc13–Cdc2 has a role in localization of Wee1 to the SPB, we observed Wee1 localization in a temperature-sensitive *cdc13-117* mutant. The *cdc13-117* cells have low levels of Cdc13 at the permissive temperatures but still enter mitosis (Booher *et al.*, 1989) (Figure 2E). We found that levels of GFP–Wee1 accumulated at the SPB at the G2/M transition were significantly reduced in the *cdc13-117* cells (Figure 2F). These results suggest that Wee1 localization to the SPB depends on Cdc13–Cdc2.

We were not able to observe Wee1 localization at the medial cortical nodes by expressing GFP–Wee1 under the control of the endogenous promoter. However, as previously reported (Moseley *et al.*, 2009), we observed localization of Wee1 at the cortical nodes, at the SPB, and in the nucleus in cells overproducing GFP–Wee1.

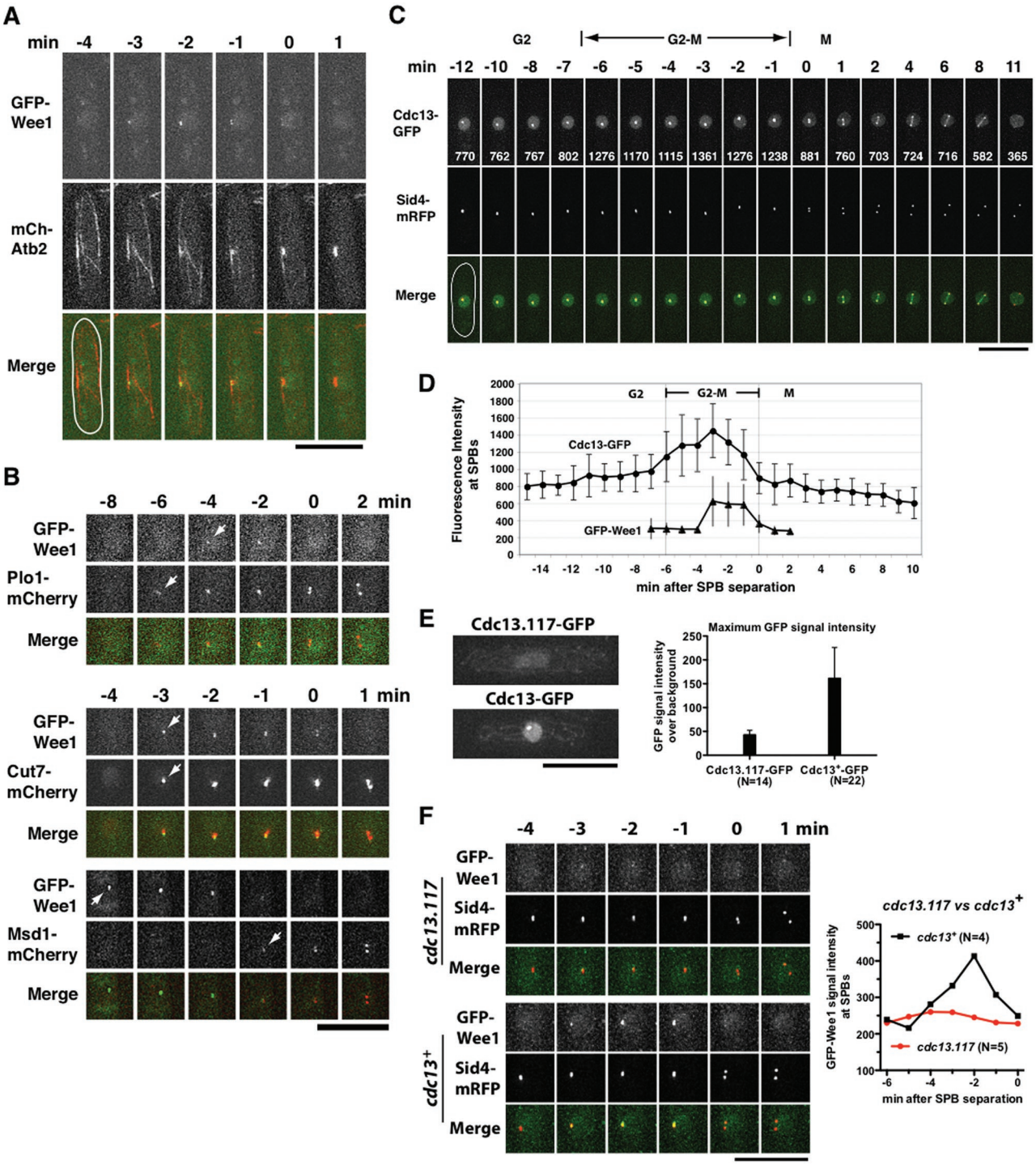

FIGURE 2: Wee1 temporally accumulates at the SPB during the G2/M transition. (A) Wee1 accumulates at the SPB when cytoplasmic microtubules are reorganized into a mitotic spindle and disappears from the SPB after spindle assembly. Live images of a cell expressing GFP–Wee1 and mCherry–Atb2 are shown. Time 0 represents when the bipolar spindle forms. (B) Timing of Wee1 accumulation at the SPB compared with mitotic proteins accumulated at the SPB. Live images of nuclear regions in cells expressing GFP–Wee1 and Plo1–mCherry, Cut7–mCherry, or Msd1–mCherry are shown. Time 0 represents when the SPBs are separated. (C) Cdc13 accumulates at the SPB in late G2 and M phase. Live cell images of cells expressing Cdc13–GFP and Sid4–mRFP are shown at 12 min before SPB separation through 11 min after SPB separation. Maximal GFP intensity at the SPB is labeled at each time point. From time 0–11 min, the average of intensities at the two SPBs is shown. (D) Quantification of Cdc13–GFP and GFP–Wee1 localized at the SPB. Average intensities of GFP signals at the SPB from cells expressing either Cdc13–GFP (N = 10) or GFP–Wee1 (N = 7) are shown as a function of time after SPB separation. Error bars show SD. (E) Cdc13 levels decrease in *cdc13.117* cells. Left, live cell images of cells expressing Cdc13.117–GFP and Cdc13–GFP. Right, quantification of Cdc13.117–GFP and Cdc13–GFP in mid-late G2 cells. Average of the maximum GFP signal intensities is shown. (F) Levels of GFP–Wee1 accumulated at the SPB during the G2/M transition are reduced in *cdc13.117* cells. Left, live cell images of a *GFP–wee1 cdc13.117* cell and a *GFP–wee1 cdc13*$^{+}$ cell; and right, quantification of GFP–Wee1 at the SPB. Bars, 10 μm.

Although Wee1 overproduction arrested cells in G2 phase, we observed mitotic entry in some cells that showed localization of Wee1 at the cortical nodes in G2 phase (indicated by the arrows in Figure 3A). Under this overproduced condition, Wee1 showed localization at the SPB in G2 phase, decreased in SPB level at the G2/M transition, then temporally increased this level, and almost disappeared from the SPB after SPB separation (Figure 3A and Supplemental Figure S1). This was consistent with the observations made under the expression condition using the endogenous promoter (Figure 1, A and E). In these cells, the Wee1 localized to the cortical nodes in G2 phase disappeared from the nodes at the G2/M transition before accumulating at the SPB (Figure 3A). To examine whether Wee1 at the cortical nodes is involved in its accumulation at the SPB, we observed Wee1 localization in *cdr2*Δ cells that do not exhibit Wee1 localization at the nodes (Moseley *et al.*, 2009). We found that Wee1 does accumulate at the SPB during the G2/M transition in *cdr2*Δ cells (Figure 3B). We also examined Wee1 localization in *cdr1*Δ cells, in which Wee1 localizes at the cortical nodes, but the Wee1 activity is not suppressed by Cdr1 (Moseley *et al.*, 2009). Wee1 also accumulated at the SPB during the G2/M transition in *cdr1*Δ cells (Figure 3B). These observations suggest that regulation of Wee1 localization and activity by Cdr2–Cdr1 is not required for Wee1 accumulation at the SPB, although it is unclear how Wee1 localized at the cortical nodes behaves in the unperturbed cell cycle.

Wee1 accumulates at the nuclear face of the SPB during the G2/M transition

To study the role of Wee1 accumulated at the SPB, we aimed to determine to which face of the SPB Wee1 is localized during the G2/M transition. During interphase, the SPB resides on the cytoplasmic surface of the nuclear envelope. During the G2/M transition, the nuclear envelope invaginates beneath the SPB and forms an opening into which the SPB settles (Ding *et al.*, 1997). After the settling, nuclear microtubules are nucleated from the nuclear face of the SPB. Thus, during the G2/M transition, the SPB has two regions facing either the nucleus or the cytoplasm.

We reasoned that if Wee1 localizes at either face of the SPB, manipulation of the levels of Wee1 present in the nucleus and in the cytoplasm would affect the levels of Wee1 accumulated at the SPB during the G2/M transition. We constructed strains harboring GFP–Wee1 tagged with two copies of SV40 nuclear localization sequence (NLSx2) (Figure 4A) and observed Wee1 localization during the G2/M transition. Levels of GFP–NLSx2–Wee1 localized at the SPB during the G2/M transition increased compared with the levels of GFP–Wee1 (Figure 4, B and C). We next constructed strains harboring GFP–Wee1 tagged with a tandem repeat of the PKI nuclear export sequence (NESx2) (Figure 4A). The levels of GFP–NESx2–Wee1 localized at the SPB decreased largely during the G2/M transition compared with the levels of GFP–Wee1 (Figure 4, B and C). These observations suggest that Wee1 accumulates at the nuclear face of the SPB during the G2/M transition.

Effects of NLS or NES tagging suggest that the NLS and NES of Wee1 may be important for the regulation of the subcellular localization of Wee1. We found two potential NLS sequences (NLS1 and NLS2) and one potential NES sequence (NES1) in Wee1 (Figure 4D). Disruption of either NLS1 or NLS2 decreased the levels of Wee1 localized at the SPB during the G2/M transition, and disruption of both was more effective for the suppression of Wee1 enrichment at the SPB (Figure 4E). In contrast, NES1 disruption increased levels of Wee1 accumulated at the SPB (Figure 4E). These results are consistent with those observed with NLS- and NES-tagged Wee1 and suggest that the nuclear import and export of Wee1 in some part may be dynamically regulated at the G2/M transition, at the timing of accumulation and disappearance of Wee1 at the nuclear face of the SPB.

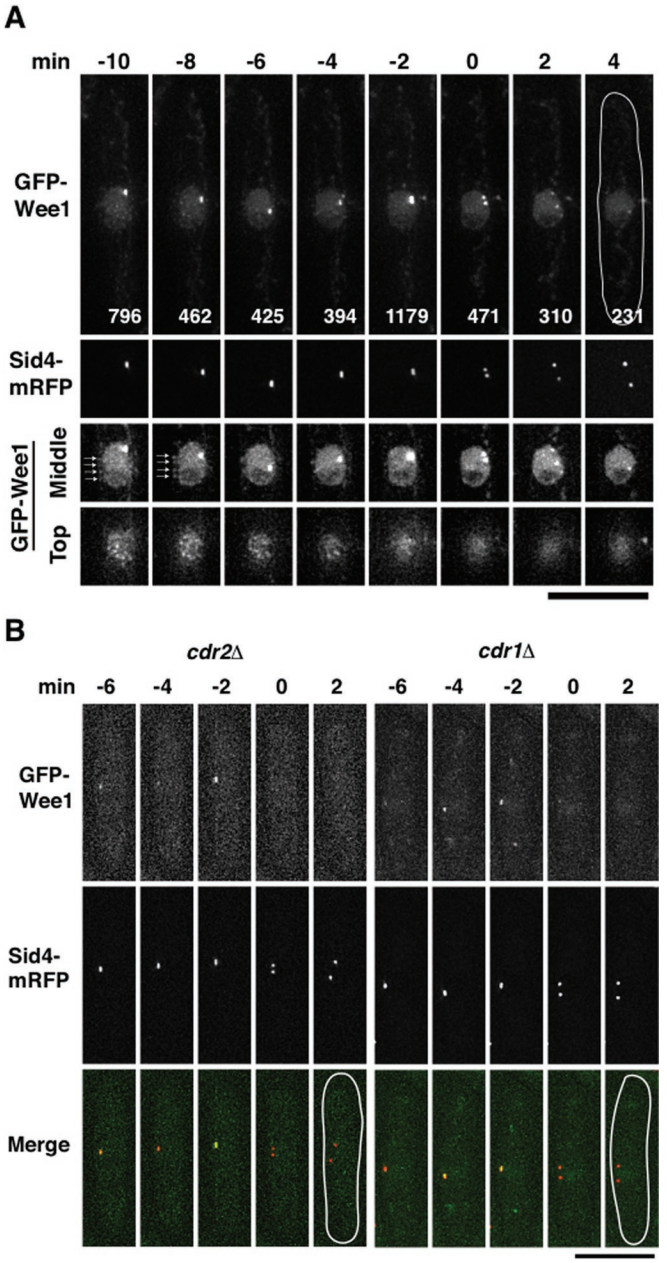

FIGURE 3: Regulation of Wee1 localization and activity by Cdr2–Cdr1 is not required for Wee1 accumulation at the SPB during the G2/M transition. (A) Levels of Wee1 localized to the cortical nodes decrease before Wee1 accumulation at the SPB. GFP–Wee1 was overproduced in the absence of thiamine using a thiamine-repressive promoter (P81nmt1) at 30°C for 20 h. The first and second rows of the panels show live images projected from 14 Z-sections 10 min before SPB separation through 4 min after SPB separation. The maximum GFP intensity at the SPB is labeled at each time point. The third and fourth rows of the panels show images from the top and the middle Z-sections. Arrows indicate GFP–Wee1 localized to the cortical nodes. (B) Wee1 accumulates at the SPB during the G2/M transition in *cdr2* deletion and *cdr1* deletion cells. Live images of a *cdr2* deletion and a *cdr1* deletion cell expressing GFP–Wee1 and Sid4–mRFP are shown from 6 min before SPB separation through 2 min after SPB separation. Bars, 10 μm.

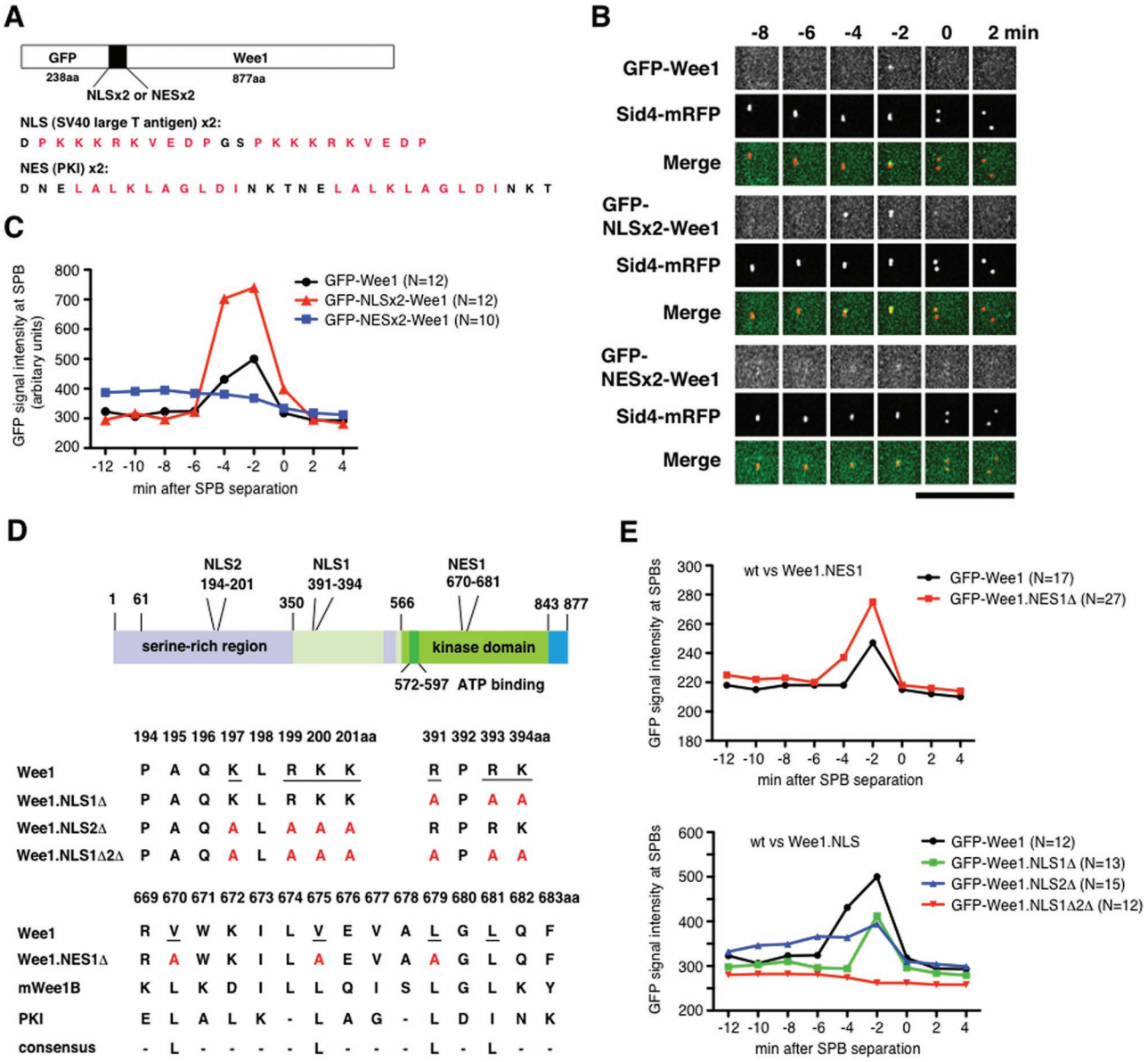

FIGURE 4: Manipulation of NLS and NES activities of Wee1 affects levels of Wee1 accumulated at the SPB during the G2/M transition. (A) Tagging of Wee1 with NLS and NES. Two copies of SV40 T antigen NLS (NLSx2) or PKI NES (NESx2) were inserted between GFP and Wee1. (B) NLS and NES tagging of Wee1 affects levels of Wee1 accumulated at the SPB. Live images of SPB regions of cells expressing GFP–Wee1, GFP–NLSx2–Wee1, and GFP–NESx2–Wee1 are shown around the time of SPB separation. (C) Quantification of NLS- and NES-tagged Wee1 accumulated at the SPB. Average of GFP signal intensity at the SPB from cells expressing GFP–Wee1 (N = 12), GFP–NLSx2–Wee1 (N = 12), and GFP–NESx2–Wee1 (N = 10) are shown. (D) Schematic representation of the structure of Wee1 showing the kinase domain, serine-rich regions, two potential NLSs, and one potential NES. Wild-type and mutated sequences of NLS1, NLS2, and NES1 are shown. NES sequences of *S. pombe* Wee1, mouse Wee1B (Oh *et al.*, 2010), and PKI are aligned. (E) Quantification of Wee1.NLS and NES mutant proteins accumulated at the SPB. Average of GFP signal intensities at the SPB are shown from cells expressing (top) GFP–Wee1 (N = 17) and GFP–Wee1.NES1Δ (N = 27) and (bottom) GFP–Wee1 (N = 12), GFP–Wee1.NLS1Δ (N = 13), GFP–Wee1.NLS2Δ (N = 15), and GFP–Wee1.NLS1Δ2Δ (N = 12).

Manipulation of NLS and NES activities of Wee1 affects cell division length

We found that cell length at mitotic entry is affected by the manipulation of NLS and NES activities of Wee1 (Figure 5, A and B; Supplemental Figure S2). In *S. pombe*, the cell length at division is regulated through a balance of Wee1 and Cdc25 activities, and the division length of *wee1* mutants is correlated with activity of Wee1 suppressing the Cdc13–Cdc2 activation in the cell (Nurse, 1990). Tagging of Wee1 with one NLS (NLSx1) or two NLSs (NLSx2) increased this length in correlation with the strength of the NLS, indicating the enhanced Wee1 activity. Cells with a disrupted Wee1 NES sequence (Wee1.NES1Δ) also divided at longer cell lengths. On the contrary, tagging of Wee1 with a tandem repeat of NES (NESx2) decreased cell division length, indicating the reduced Wee1 activity. The disruption of NLS sequences of Wee1 also decreased cell division length; the cells with two NLSs disrupted (Wee1.NLS1Δ2Δ) dividing at a shorter cell length compared with a single NLS. Tagging of Wee1.NLS1Δ2Δ with NESx2 further decreased cell

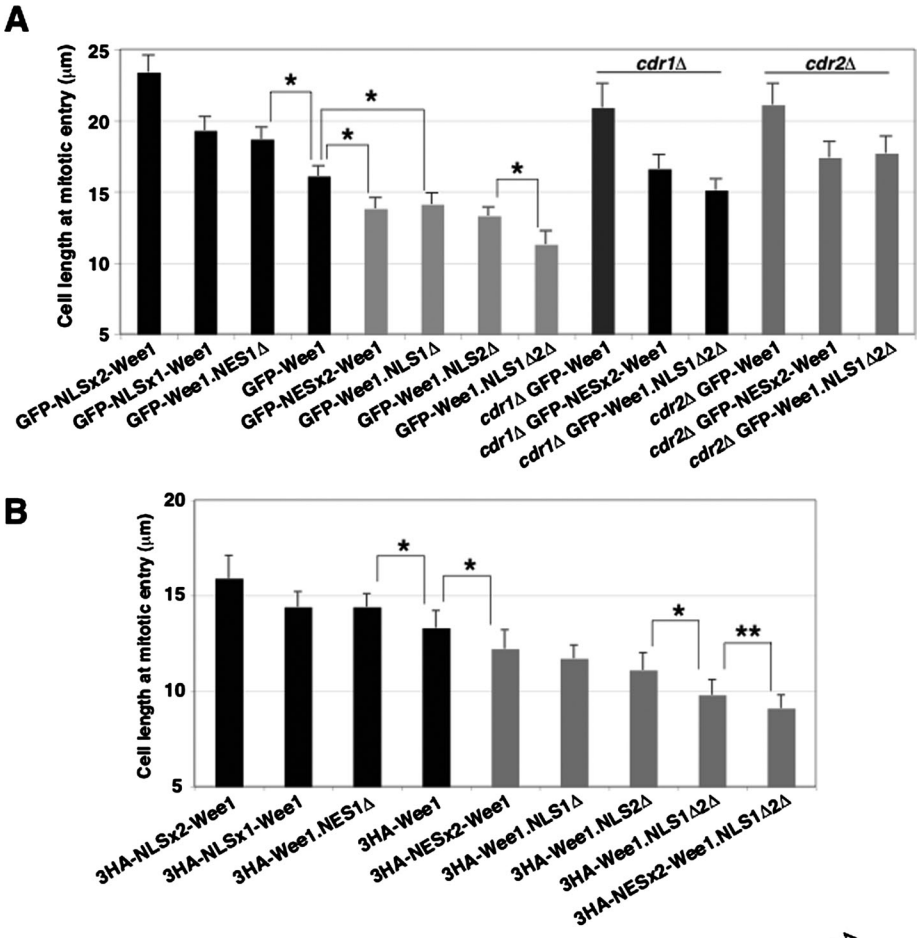

FIGURE 5: Manipulation of NLS and NES activities of Wee1 affects cell length at mitotic entry. (A) Average cell lengths at SPB separation are shown from cells expressing GFP–NLSx2–Wee1 (N = 27), GFP–NLSx1–Wee1 (N = 18), GFP–Wee1.NES1Δ (N = 11), GFP–Wee1 (N = 38), GFP–NESx2–Wee1 (N = 16), GFP–Wee1.NLS1Δ (N = 17), GFP–Wee1.NLS2Δ (N = 22), GFP–Wee1.NLS1Δ2Δ (N = 12), GFP–Wee1 *cdr1*Δ (N = 71), GFP–NESx2–Wee1 *cdr1*Δ (N = 38), GFP–Wee1.NLS1Δ2Δ *cdr1*Δ (N = 15), GFP–Wee1 *cdr2*Δ (N = 24), GFP–NESx2–Wee1 *cdr2*Δ (N = 33), and GFP–Wee1.NLS1Δ2Δ *cdr2*Δ (N = 36). Error bars show SD. *$p < 0.0001$ from Student's *t* test. (B) Average cell lengths at SPB separation are shown from cells expressing 3HA–NLSx2–Wee1 (N = 33), 3HA–NLSx1–Wee1 (N = 28), 3HA–Wee1.NES1Δ (N = 33), 3HA–Wee1 (N = 26), 3HA–NESx2–Wee1 (N = 34), 3HA–Wee1.NLS1Δ (N = 29), 3HA–Wee1.NLS2Δ (N = 30), 3HA–Wee1.NLS1Δ2Δ (N = 26), and 3HA–NESx2–Wee1.NLS1Δ2Δ (N = 33). Error bars show SD. *$p < 0.0001$ and **$p = 0.0002$ from Student's *t* test, respectively. (C) Quantification of Wee1 protein levels in 3HA-tagged Wee1 mutant cells. A typical example of immunoblot analysis from *3HA–wee1* mutant cells is shown. Wee1 and α-tubulin were detected using anti-HA and anti–α-tubulin antibodies, respectively. Average Wee1 protein levels (±SD; N = 3) are indicated as ratios to 3HA–Wee1 levels.

division length (Figure 5B). These results show that the increase in levels of nuclear Wee1 results in the increase in both Wee1 kinase activity to suppress Cdc13–Cdc2 and Wee1 levels enriched at the SPB during the G2/M transition. On the contrary, the decrease in levels of nuclear Wee1 results in the decrease in both Wee1 kinase activity to suppress Cdc13–Cdc2 and Wee1 levels at the SPB.

Our results could be explained from two models. In one model, Wee1 could inhibit Cdc13–Cdc2 more efficiently in the nucleus than in the cytoplasm, and increase and decrease in levels of nuclear Wee1 would lead to higher and lower levels of suppression of Cdc13–Cdc2, respectively. In the other model, Wee1 could inhibit Cdc13–Cdc2 both in the nucleus and in the cytoplasm with a similar efficiency, and the changes in Wee1 localization would lead to the changes in total Wee1 protein levels in the cell by affecting the stability of Wee1. Thus increase and decrease of nuclear Wee1 levels would result in increase and decrease of total Wee1 levels, respectively. To explore these two possibilities, we measured by immunoblot analysis Wee1 protein levels in cells expressing three tandem repeats of the influenza virus hemagglutinin epitope (3HA)–Wee1 with altered NLS and NES activities (Figure 5C). We found that Wee1 protein levels in the cells dividing at longer lengths with the apparent increased Wee1 activity (Wee1.NES1Δ, NLSx1–Wee1, and NLSx2–Wee1) were similar or slightly reduced compared with those in wild-type 3HA–Wee1 cells. On the contrary, in the cells dividing at shorter lengths with the apparent decreased Wee1 activity (NESx2–Wee1, Wee1.NLS1Δ, Wee1.NLS2Δ, Wee1.NLS1Δ2Δ, and NESx2–Wee1.NLS1Δ2Δ), Wee1 was similar or rather increased in levels. Especially, Wee1 were increased by 40–60% in the cells with a *wee1.NLS2*Δ mutation (Wee1.NLS2Δ, Wee1.NLS1Δ2Δ, and NESx2–Wee1.NLS1Δ2Δ), suggesting that increase in Wee1 level in the cytoplasm does not increase the suppression level for Cdc13–Cdc2. These results are consistent with the former model and suggest that the changes in Wee1 localization, but not in total Wee1 protein levels, are responsible for the changes in division length of cells expressing Wee1 with altered NLS and NES activities.

Because Wee1 seems to be inactivated by Cdr1–Cdr2 localized at the cortical nodes (Martin and Berthelot-Grosjean, 2009; Moseley *et al.*, 2009), manipulation of the NLS and NES activities of Wee1 may affect cell division length through altering the levels of Wee1 inactivated by Cdr1–Cdr2. We

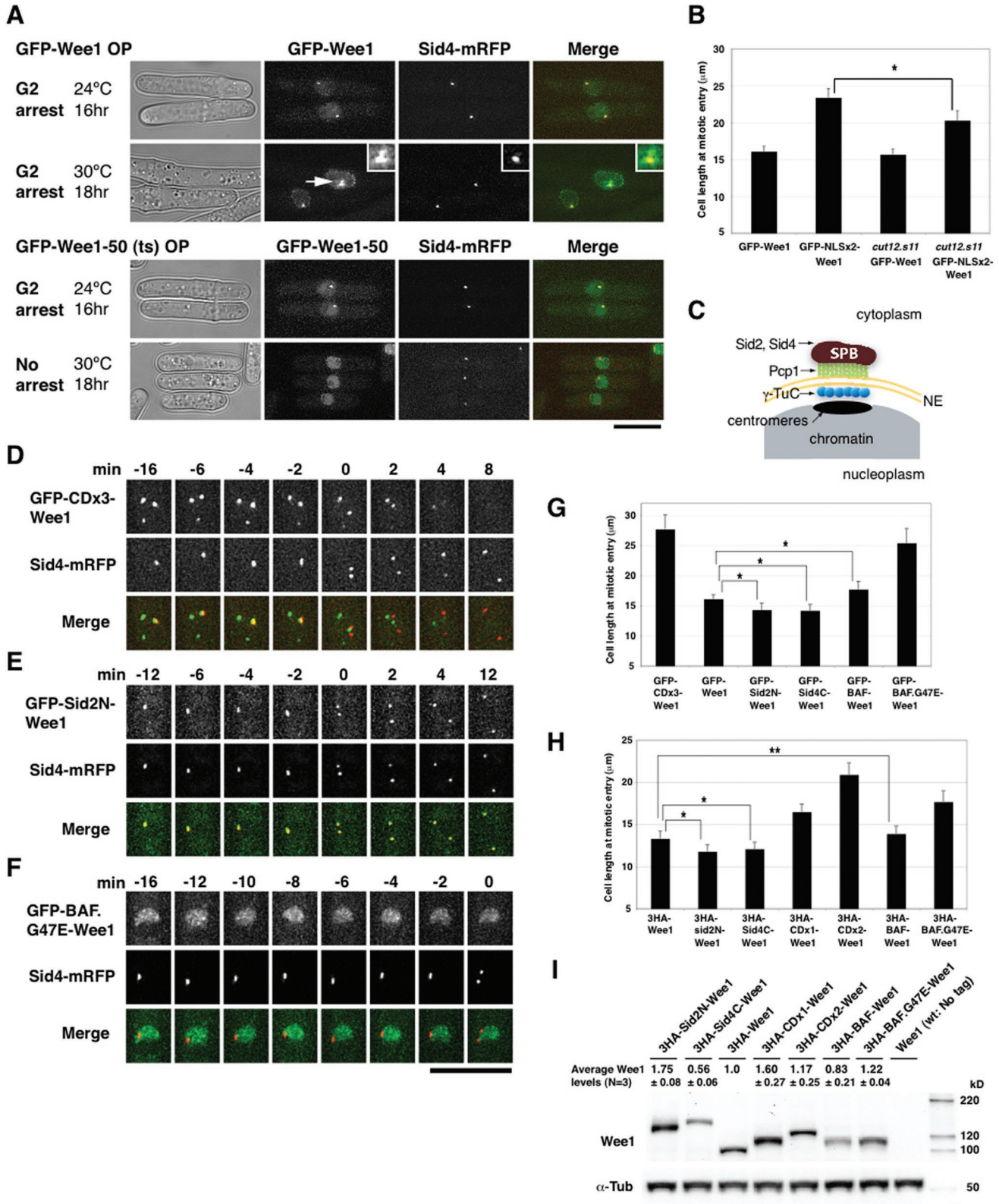

FIGURE 6: Nuclear Wee1 effectively controls cell division length around the SPB. (A) Localization of Wee1-50 around the SPB correlates with the ability of Wee1-50 to induce a G2 arrest. GFP–Wee1-50 was overexpressed in the absence of thiamine under the control of a thiamine-repressive promoter (P3nmt1) at the permissive temperature (24°C) for 16 h and at the semipermissive temperature (30°C) for 18 h in cells expressing an endogenous wild-type *wee1*$^+$ gene. Note that GFP–Wee1-50 does not induce cell elongation much at 30°C or Wee1-50 accumulation to the SPB. Inset, one of the SPB regions (arrow) is enlarged to show that another nuclear dot is formed close to the SPB. (B) The *cut12.s11* mutation partially suppresses the effect of NLSx2–Wee1 on cell division length. The average cell lengths at SPB separation are shown from cells expressing GFP–Wee1 (N = 38) and GFP–NLSx2–Wee1 (N = 15) and from *cut12.s11* cells expressing

examined whether the Wee1 mutations affect cell division length without Cdr1–Cdr2 activities. We found that the double-mutant cells *cdr1Δ NESx2–wee1*, *cdr1Δ wee1.NLS1Δ2Δ*, *cdr2Δ NESx2–wee1*, and *cdr2Δ wee1.NLS1Δ2Δ* divided at shorter cell lengths compared with single-mutant *cdr1Δ* and *cdr2Δ* cells (Figure 5A), showing that levels of nuclear Wee1 affect cell division length independently of Cdr1–Cdr2 activities.

Nuclear Wee1 efficiently controls cell division length around the SPB

As shown above, there is a correlation between the cell length at mitotic entry and levels of Wee1 at SPB during the G2/M transition. We observed that the level of GFP–Wee1 localized at the SPB decreased before it accumulated during the G2/M transition both in cells expressing GFP–Wee1 with an endogenous promoter and in cells overproducing GFP–Wee1 (Figures 1 and 3A; Supplemental Figure S1). Thus, when Cdc13–Cdc2 levels at the SPB began to increase, the levels of GFP–Wee1 were reduced at the SPB (Figure 2D). These observations suggest that the regulation of Wee1 level at the SPB in late G2 phase may play a role in the mechanism of Cdc13–Cdc2 activation. To explore this possibility further, we overproduced the GFP-tagged version of a temperature-sensitive Wee1 mutant protein, Wee1-50 (Nurse, 1990), at the permissive temperature (24°C) and semipermissive temperature (30°C) and examined cell length and localization of the protein. GFP–Wee1-50 induced a G2 arrest, and the protein localized to the SPB and in the nucleus at 24°C, whereas it did not induce either a G2 arrest or Wee1 accumulation to the SPB at 30°C (Figure 6A). When wild-type Wee1 was overproduced as a control, Wee1 localized to the SPB and in the nucleus at both temperatures (Figure 6A). These results suggest that the localization of Wee1 to the SPB may be required for the suppression of Cdc13–cdc2 activity. Additionally, we found that when Wee1 was overproduced at higher levels, it started to form nuclear foci at regions other than the SPB (Figure 6A, arrow and inset), and eventually two or more foci became apparent in the nucleus. This observation suggests that Wee1 accumulates at the nuclear periphery adjacent to the SPB, but not the cytoplasmic side of the SPB in late G2 phase.

To confirm that Wee1 has a role at the SPB in the mechanism of Cdc13–Cdc2 activation, we examined the effect of *cut12.s11* mutation on cell division length. A dominant mutant allele of an SPB component Cut12, *cut12.s11*, suppresses the phenotype of *cdc25* mutant cells by prematurely recruiting Polo kinase Plo1 to the SPB during interphase to compensate for the reduction of Cdc25 activity (MacIver *et al.*, 2003; Hagan, 2008). We found that although the *cut12.s11* mutation did not affect division length of wild-type cells, it partially suppressed the effect of NLSx2–Wee1 on cell division length (Figure 6B). This suggests that Wee1 has some role at the SPB in suppressing Cdc13–Cdc2 activation.

We next tested whether targeting of Wee1 to the nuclear periphery adjacent to the SPB affects cell division length. We used the chromodomain (CD) of Swi6 to target Wee1 to the centromeres that are discretely clustered at the nuclear periphery adjacent to the SPB (Figure 6C) (Funabiki *et al.*, 1993). The CD binds to Lys-9–methylated histone H3, largely locating at the pericentromeric heterochromatin regions (Kitajima *et al.*, 2006). Wee1 tagged with three copies of CD (GFP–CDx3–Wee1) was dominantly localized around the SPB and additional one to three regions in the nucleus during interphase (Figure 6D). GFP–CDx3–Wee1 remained around the SPB during the G2/M transition, then detached from the SPB after spindle assembly, and disappeared during prometaphase. The cells divided at much longer cell lengths compared with wild-type cells (Figure 6G, see GFP–Wee1). We then targeted Wee1 to the cytoplasmic face of the SPB as a control: We fused an N-terminal fragment (1–207 aa) of Sid2 (Sid2N) or C-terminal fragment (301–660 aa) of Sid4 (Sid4C) to the N terminus of Wee1 in order to target Wee1 to the cytoplasmic face of the SPB (Figure 6C). Sid2 and Sid4 are SPB components localized at the cytoplasmic face to control cytokinesis and septum formation (Sparks *et al.*, 1999; Chang and Gould, 2000). Sid2N and Sid4C are shown to localize at the SPB through the cell cycle (Tomlin *et al.*, 2002; Morrell *et al.*, 2004). We found that GFP–Sid2N–Wee1 (Figure 6E) and GFP–Sid4C–Wee1 (Supplemental Figure S3) were localized to the SPB throughout the cell cycle at relatively constant levels, and the temporal accumulation of Wee1 at the SPB was not observed during the G2/M transition. The cells expressing the fusion proteins divided at shorter cell lengths (Figure 6G). Thus targeting of Wee1 to the nuclear periphery adjacent to the SPB, but not to the cytoplasmic side of the SPB, is effective for suppressing cell division.

We measured Wee1 protein levels in the Wee1-targeting cells and found that Wee1 levels were increased in CDx1– and CDx2–Wee1 cells and in Sid2N–Wee1 cells but were decreased in Sid4C–Wee1 cells (Figure 6I). Considering that cells expressing nuclear Wee1 (CDx1– and CDx2–Wee1) divide at longer cell lengths, and cells expressing cytoplasmic Wee1 (Sid2N–Wee1 and Sid4C–Wee1) divide at shorter cell lengths, cell division length is correlated to Wee1 localization but not to total Wee1 protein levels. These results also suggest that the suppression of cell division in CD-tagged cells could result from either Wee1 accumulation to

GFP–Wee1 (N = 40) and GFP–NLSx2–Wee1 (N = 40). *$p < 0.0001$ from Student's *t* test. (C) Schematic drawing of Wee1-targeting sites. Wee1 was targeted to the centromere regions that are clustered around the nuclear periphery adjacent to the SPB, the cytoplasmic face of the SPB and chromatin, using the chromodomain (CD) of Swi6; an N terminus of Sid2 and a C terminus of Sid4; and human BAF, respectively. Positions of an SPB component Pcp1 and the γ-tubulin complex (γ-TuC) are also shown. (D) GFP–CDx3–Wee1 localizes as nuclear dots including the region close to the SPB in G2 phase, detaches from the SPB after spindle assembly, and disappears during prometaphase. (E) GFP–Sid2N–Wee1 localizes to the SPB throughout the cell cycle. SPB localization of the fusion protein is shown from late G2 through early anaphase. (F) GFP–BAF.G47E–Wee1 localizes to the hemisphere- or crescent-shaped chromatin region in the nucleus. The fusion protein does not accumulate at the SPB during the G2/M transition. (G) Average cell lengths at SPB separation of cells expressing GFP–Wee1 (N = 38), GFP–CDx3–Wee1 (N = 18), GFP–Sid2N–Wee1 (N = 26), GFP–Sid4C–Wee1 (N = 14), GFP–BAF–Wee1 (N = 38), and GFP–BAF.G47E–Wee1 (N = 30). Bars represent SD. *$p < 0.0001$ from Student's *t* test. (H) Average cell lengths at SPB separation of cells expressing 3HA–Wee1 (N = 26), 3HA–Sid2N–Wee1 (N = 35), 3HA–Sid4C–Wee1 (N = 42), 3HA–CDx1–Wee1 (N = 37), 3HA–CDx2–Wee1 (N = 36), 3HA–BAF–Wee1 (N = 42), and 3HA–BAF.G47E–Wee1 (N = 36). Bars represent SD. *$p < 0.0001$ and **$p = 0.0067$ from Student's *t* test, respectively. (I) Quantification of Wee1 protein levels in Wee1-targeting mutant cells. A typical example of immunoblot analysis from *3HA–wee1*-targeting cells is shown. Wee1 and α-tubulin were detected using anti-HA and anti–α-tubulin antibodies, respectively. Average Wee1 protein levels (±SD; N = 3) are shown as ratios to 3HA–Wee1 levels.

the nuclear periphery adjacent to the SPB, increase in total nuclear Wee1 level, or a combination of both.

To study whether Wee1 accumulation around the SPB is essential for the suppression of cell division, we created the condition in which Wee1 is localized in the nucleus but not enriched at the SPB during the G2/M transition. Wee1 was targeted to chromatin using human barrier-to-autointegration factor (BAF), an inner nuclear envelope protein with DNA-binding activity (Lee and Craigie, 1998; Haraguchi *et al.*, 2008). When expressed at low levels in *S. pombe* cells, BAF was localized to chromatin. Targeting of Wee1 to chromatin using either wild-type BAF or a mutant BAF.G47E, which shows higher chromatin-binding activity (Segura-Totten *et al.*, 2002), was effective for immobilizing Wee1 and suppressing the accumulation of Wee1 at the SPB during the G2/M transition (Figure 6F and Supplemental Figure S4). Cells expressing BAF.G47E–Wee1 showed higher levels of Wee1 localization to chromatin and divided at longer cell lengths compared with cells expressing BAF–Wee1 (Figure 6G). These results suggest that the ability of Wee1 to accumulate around the SPB is not essential for suppressing cell division, and increasing the levels of nuclear Wee1 is sufficient for the suppression.

Wee1 acts at the nuclear face of the SPB as a regulator of the G2/M transition

We sought to determine the role of Wee1 accumulated at the nuclear side of the SPB during the G2/M transition. Wee1 may be involved in the regulation of spindle assembly, as the SPB nucleates spindle microtubules at the nuclear side. To explore this possibility, we constructed double-mutant cells of *wee1* localization mutants with a *pcp1-18* temperature-sensitive mutant and examined the phenotypes. Pcp1 is an evolutionarily conserved pericentrin-related protein that localizes to the inner plaque of the SPB throughout the cell cycle (Flory *et al.*, 2002). The *pcp1-18* mutant cells are defective in the recruitment of Polo kinase Plo1 to the SPB and bipolar spindle formation at the restrictive temperature (Fong *et al.*, 2009). The *pcp1-18* ts phenotype is partially suppressed by *wee1-50*, a temperature-sensitive *wee1* mutant (Nurse, 1990), suggesting that the defect in Plo1 recruitment to the SPB is partially suppressed by reducing the Wee1 activity in the cell (Fong *et al.*, 2009). We reasoned that Wee1 enriched at the nuclear face of the SPB may be responsible for the regulation of Cdc2 kinase activity by counteracting Plo1 and that reducing the level of Wee1 at the nuclear face of the SPB may suppress the phenotypes of *pcp1-18*. As expected, the temperature sensitivity of *pcp1-18* cells was partially suppressed by reducing Wee1 levels at the nuclear side using *wee1.NLS1*Δ*2*Δ mutation and enhanced by increasing Wee1 levels at the nuclear side using *wee1.NES1*Δ mutation (Figure 7A).

To confirm the role of Wee1 during the G2/M transition in addition to its role in late G2, we constructed a *wee1.as1* strain, in which Wee1 kinase activity is suppressed by the addition of a PP1 analogue, 4-amino-1-(*tert*-butyl)-3-(1′-naphthylmethyl)pyrazolo[3,4-*d*] pyrimidine (1-NM-PP1) (Bishop *et al.*, 2000). As expected from Wee1 functioning as a negative regulator of the Cdc13–Cdc2, Wee1 inactivation by the analogue accelerated mitotic entry in *wee1.as1* cells (Supplemental Figure S5). We found that Wee1 was no longer enriched at the SPB during the G2/M transition (Figure 7B), showing that kinase activity is required for Wee1 localization to the SPB. We constructed *wee1.as1 pcp1-18* double-mutant cells and observed the phenotypes at the restrictive temperature in the presence and absence of the analogue (Figure 7C). In the absence of the analogue, they showed the phenotype of *pcp1-18* single-mutant cells; thus they were defective in spindle formation. In the presence of the analogue, however, many of the double-mutant cells formed a bipolar spindle. These results support that Wee1 has a role in regulating spindle assembly by suppressing Cdc2 kinase activity during the G2/M transition.

DISCUSSION

We demonstrated here by live cell imaging that Wee1 is highly dynamic at the SPB around the G2/M transition. Wee1 accumulates at the SPB when Cdc13–Cdc2 peaks at the SPB and disappears from the SPB during spindle assembly when Cdc13–Cdc2 decreases at the SPB to the levels of late G2 phase. This dynamic behavior of Wee1 at the SPB seems to be important for the regulation of Cdc13–Cdc2 activity and entry into mitosis.

We showed that the balance of nuclear and cytoplasmic Wee1 affects the activity of Wee1 to negatively regulate mitotic entry. When the nuclear levels of Wee1 increase, the cells divide at longer cell lengths, suggesting that Cdc13–Cdc2 activity is regulated mainly in the nucleus. This is consistent with the finding that the Cdc13–Cdc2 complex localizes mostly in the nucleus and to the SPB at late G2 phase (Decottignies *et al.*, 2001). In mammalian cells, translocation of Wee1 from the nucleus to the cytoplasm seems to be important for regulating cyclin B1–Cdk1 activity (Baldin and Ducommun, 1995; Oh *et al.*, 2010). In *S. pombe*, a major change in levels of Wee1 occurs at the SPB during late G2 through early M phase. This change is accompanied by the change in levels of Cdc13–Cdc2 accumulated at the SPB. We also showed here that the localization of Wee1 around the SPB is correlated with the ability of Wee1 to induce a G2 arrest and that targeting of Wee1 to the nuclear periphery adjacent to the SPB increases cell division length. It is tempting to speculate that the Cdc13–Cdc2 activity is efficiently regulated by nuclear Wee1 around the SPB. We propose that Cdc13–Cdc2 activity is controlled both by regulating Wee1 kinase activity through the Pom1–Cdr2–Cdr1 signaling pathway (Martin and Berthelot-Grosjean, 2009; Moseley *et al.*, 2009) and by regulating Wee1 localization around the SPB.

As shown here, the dynamic behavior of Wee1 at the SPB may be regulated by the NLS and NES activities of Wee1. Alternatively, the affinity of nuclear Wee1 with the SPB, but not the NLS and NES activities of Wee1, may be regulated during the G2/M transition. One of the Wee1-binding partner candidates at the SPB is its substrate Cdc13–Cdc2. We observed that the kinase activity of Wee1 is required for Wee1 accumulation at the SPB during the G2/M transition. This suggests that the interaction of Wee1 with its substrate is important for the recruitment of Wee1 to the SPB. The interaction of Wee1 and cyclin B1–Cdk1 with low kinase activities has been recently shown using human somatic cell extracts (Deibler and Kirschner, 2010). Wee1 localization to the SPB may result from a similar interaction between Wee1 and Cdc13–Cdc2, as Cdc13–Cdc2 is highly enriched at the SPB during the G2/M transition when the complex is not fully activated. We have shown here using a *cdc13* mutant that Wee1 localization to the SPB depends on Cdc13–Cdc2. Whether Wee1 binds directly to Cdc13–Cdc2 at the SPB and how this interaction is regulated remains to be determined.

Our observations show that Wee1 functions in suppressing Cdc13–Cdc2 during the G2/M transition as well as in late G2. When the SPB is embedded in the nuclear envelope during the G2/M transition, two regions of the SPB facing either the nucleus or the cytoplasm have distinct functions. Proteins involved in spindle assembly are localized at the nuclear face of the SPB. Our results are consistent with the hypothesis that Wee1 accumulates at the nuclear face of the SPB during the G2/M transition and functions in regulating spindle assembly (Figure 8). We showed that manipulations that increased the levels of nuclear Wee1 increase

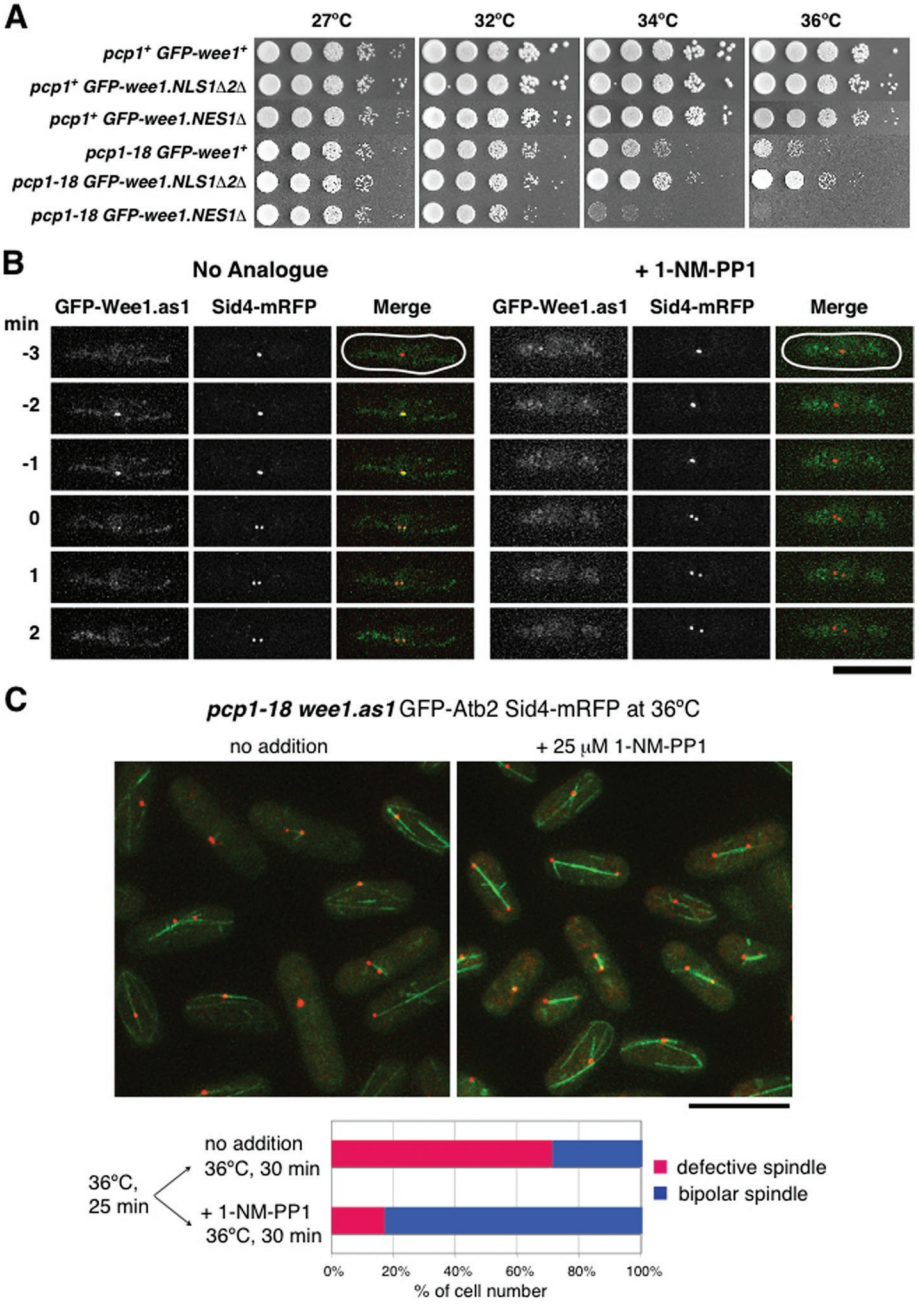

FIGURE 7: The mitotic defect of *pcp1-18* cells is partially suppressed by *wee1.NLS1Δ2Δ* mutation or Wee1 inactivation and enhanced by *wee1.NES1Δ* mutation. (A) Tenfold serial dilution assays of *pcp1-18 wee1* double-mutant cells on rich YES media. The plates were incubated at 27, 32, 34, or 36°C for 2 d. (B) Kinase activity is required for accumulation of Wee1 at the SPB. Live images of cells expressing GFP–Wee1.as1 in the presence or absence of 1-NM-PP1 are shown. Note that in the presence of 1-NM-PP1, GFP–Wee1.as1 does not accumulate at the SPB during the G2/M transition. (C) Bipolar spindle assembly is partially restored in *pcp1-18 wee1.as1* cells at the restrictive temperature in the presence of 1-NM-PP1. The *pcp1-18 wee1.as1* cells expressing GFP–Atb2 and Sid4–mRFP were incubated at 36°C for 25 min, incubated further in the presence or absence of 25 μM 1-NM-PP1 at 36°C for 30 min, and fixed for microscopy. Bars, 10 μm.

the levels of Wee1 recruited to the SPB, whereas manipulations that increased the levels of cytoplasmic Wee1 decrease the Wee1 levels at the SPB. We also showed that the defect in spindle assembly of an SPB component *pcp1-18* mutant is partially suppressed by reducing the levels of Wee1 at the nuclear face of the SPB and exacerbated by increasing the Wee1 levels at the nuclear face. The *pcp1-18* cells exhibit a defect in Plo1 recruitment to the SPB (Fong *et al.*, 2009), which seems to be required for a positive feedback loop to fully activate the Cdc13–Cdc2 complex by counteracting Wee1 (Hagan, 2008). Reducing the levels of Wee1 at the nuclear face of the SPB seems to compensate the loss of the Plo1-dependent positive feedback loop (Figure 8). Our previous observation that disturbing the function of the nuclear γ-tubulin complex arrests cells at the G2/M transition in a Wee1-dependent manner (Masuda *et al.*, 2006a) also suggests a role of Wee1 in the regulation of spindle assembly. We propose that Wee1 functions at the nuclear face of the SPB to locally regulate the activity of Cdc13–Cdc2, which could be important for suppressing spindle assembly until Cdc13–Cdc2 is highly activated through the Plo1-dependent positive feedback loop.

The *pcp1-18* cells also show a defect in SPB insertion into the nuclear envelope. Cdc13–Cdc2 activation through the Plo1-dependent positive feedback loop seems to be required for SPB insertion (Fong *et al.*, 2009). Cut12, an SPB component localized at the nuclear side of the SPB, is also proposed to function in the local activation of Cdc13–Cdc2 that induces SPB insertion (Tallada *et al.*, 2009). Our results suggest that, during the G2/M transition, nuclear Wee1 has access to the nuclear face of the SPB that resides on the cytoplasmic surface of the nuclear envelope and suppresses or exacerbates the phenotype of *pcp1-18* dependent on the levels (Figure 8). They also suggest that there must be a mechanism that locally changes the protein transport activity or permeability of the nuclear envelope beneath the SPB before its invagination of the nuclear envelope and insertion. The change in property of the nuclear envelope beneath the SPB seems to be one of the initial events at the G2/M transition, which could be induced by the low activation levels of Cdc13–Cdc2 and should be important to integrate the signals from the cytoplasm and the nucleus at the SPB to further advance mitotic entry.

In mammalian cells, cyclin B–Cdk1 is progressively activated in prophase, and different thresholds of the activity trigger specific mitotic events in prophase (Lindqvist *et al.*, 2007; Gavet and Pines, 2010). At early prophase when cyclin B–Cdk1 activity is low, the cells reversibly return back to the end of the G2 phase called "antephase" on exposure to stress such as lack of microtubule function and DNA damage (Matsusaka and Pines, 2004; reviewed in Chin and Yeong, 2010). These observations suggest that the progressive activation of

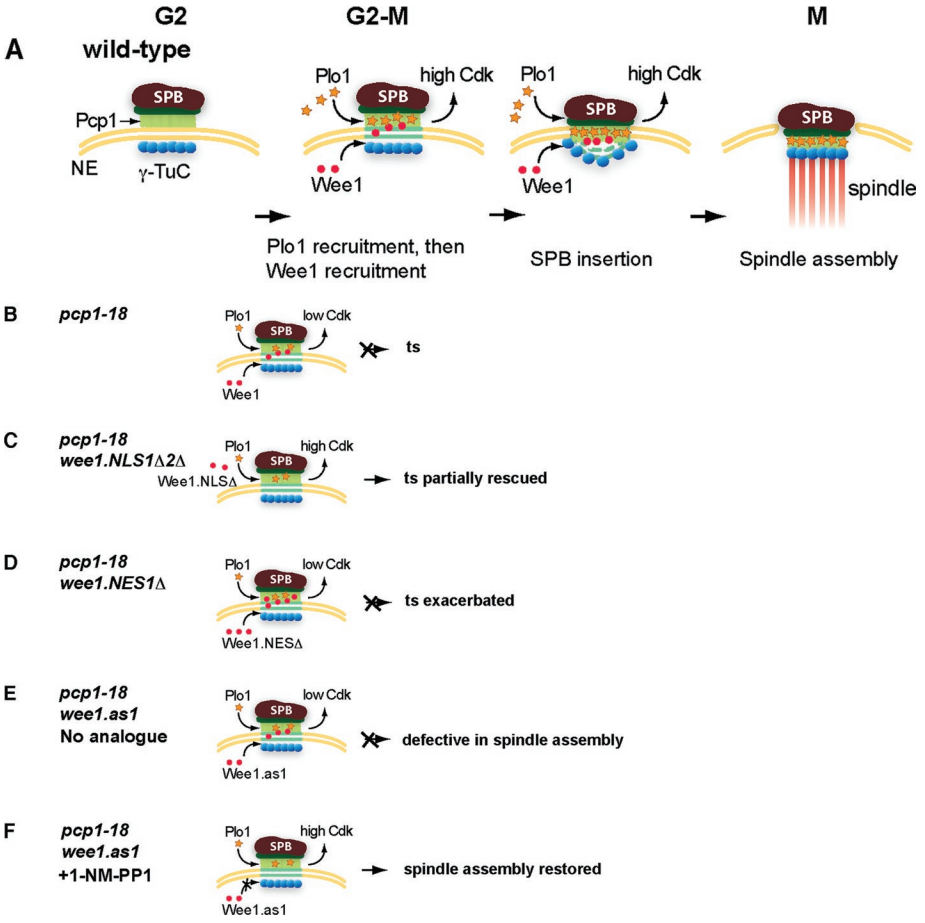

FIGURE 8: Model for the role of Wee1 at the nuclear face of the SPB in the G2/M transition. (A) During the G2/M transition, Plo1 and then Wee1 accumulate at the nuclear face of the SPB that resides on the cytoplasmic surface of the nuclear envelope. The property of the nuclear envelope beneath the SPB is changed so that nuclear Wee1 has access to the nuclear face of the SPB. Wee1 counteracts a Plo1-dependent positive feedback loop for Cdc13–Cdc2 activation. When the Plo1 activity is high enough to overcome the Wee1 activity, Cdc13–Cdc2 is fully activated for SPB insertion and spindle formation. (B) The *pcp1-18* mutant is defective in the recruitment of Plo1 to the SPB, SPB insertion, and spindle assembly at the restrictive temperature. (C, D) The temperature sensitivity of *pcp1-18* is partially rescued by a wee1 mutation reducing Wee1 levels at the nuclear face of the SPB (C) and exacerbated by a wee1 mutation increasing Wee1 levels at the nuclear face (D). (E, F) Spindle assembly is restored in *pcp1-18 wee1.as1* cells by Wee1 inactivation with 1-NM-PP1.

cyclin B–Cdk1 may be crucial for both positively and negatively regulating mitotic progression at prophase. In *S. pombe* cells, the progressive activation of Cdc13–Cdc2 seems to be achieved during the G2/M transition by regulating the timing of SPB localization of Cdc13–Cdc2; Plo1, a positive regulator; and Wee1, a negative regulator. We propose that spatiotemporal regulations of Wee1 and other cell cycle regulators around the SPB during the G2/M transition are crucial for proper mitotic entry and progression.

MATERIALS AND METHODS

Yeast methods and strains

The *S. pombe* strains used in this study are listed in Table 1. Fission yeast media, growth conditions, and manipulations were carried out as previously described (Moreno *et al.*, 1991). Cells were grown in yeast extract and supplements (YES) media before live cell imaging. For overproduction of Wee1 using thiamine-repressive promoters, cells grown in YES were transferred to Edinburgh minimal medium 2 (EMM2) supplemented with amino acids in the absence of thiamine and incubated at 30°C for 18–20 h or at 24°C for 16 h.

Fluorescent protein fusion constructs

GFP–Wee1 fusion constructs were made by two methods as follows: 1) The nmt1 promoter of pCST3 (Chikashige *et al.*, 2004) was replaced with the promoter region of *wee1*$^+$ at the *Pst*I/*Nde*I sites, the sequence encoding GFP–S65T was ligated at the *Bam*HI/*Xho*I sites, and the entire coding region of the *wee1*$^+$ gene was ligated in frame to the 3′ end of GFP–S65T at the *Xho*I/*Bgl*II sites. To construct strains carrying GFP–Wee1.NES1Δ, GFP–Wee1.NLS1Δ, GFP–Wee1.NLS2Δ, and GFP–Wee1.NLS1Δ2Δ, *wee1* mutant genes were created by PCR-based site-directed mutagenesis before integration of the genes at the *Xho*I/*Bgl*II sites. The resulting plasmids, pHRM1GFP–Wee1 and other pHRM1GFP–Wee1 mutants, were integrated into the chromosome at the *lys1* gene locus of cells with a *wee1* deletion background. 2) The promoter region of *wee1*$^+$ was PCR amplified and inserted at the *Bam*HI site between a selection marker *kanR* and GFP–S65T of pCSS25 vector. Using the plasmid as a template, the authentic *wee1*$^+$ gene was replaced with *GFP–wee1* by a PCR-based gene targeting method (Bähler *et al.*, 1998).

To construct strains carrying GFP–NLSx2–Wee1, GFP–NLSx1–Wee1, and GFP–NESx2–Wee1, oligonucleotides harboring a tandem repeat of SV40 NLS, a single SV40 NLS, and a tandem repeat of PKI NES were ligated in frame, respectively, at the *Xho*I site between GFP.S65T and Wee1 of pHRM1GFP–Wee1 plasmid. To construct strains carrying GFP–Sid2N–Wee1, GFP–Sid4C–Wee1, GFP–CDx3–Wee1, GFP–BAF–Wee1, and GFP–BAF.G47E–Wee1, Sid2 (1–207 aa), Sid4 (301–660 aa), Swi6 (69–143 aa), and human BAF and BAF.G47E cDNA were PCR amplified, respectively, and ligated in frame at the *Xho*I site of pHRM1GFP–Wee1. Occasional self-ligations of CD fragments resulted in the plasmids harboring one to three copies of CD. The resulting plasmids were integrated at the *lys1* locus of *wee1* deletion cells. To construct the strain carrying GFP–Wee1 under the control of the P81nmt1 promoter, the coding sequence of *wee1*$^+$ was ligated at the *Xho*I/*Bgl*II site of pCSU72 (Chikashige *et al.*, 2004).

Strains carrying Cdc13–GFP, Cdc13.117–GFP, Plo1–mCherry, Cut7–mCherry, and Msd1–mCherry were constructed by replacing the *cdc13*$^+$, *cdc13.117*, *plo1*$^+$, *cut7*$^+$, and *msd1*$^+$ genes, respectively, with the tagged genes and a selection marker nourseothricin-dihydrogen sulfate (clonNAT)–resistant gene (*natR*), kanamycin-resistant gene (*kanR*), or hygromycin B–resistant gene (*hphR*) by a PCR-based gene targeting method. To construct the strains carrying GFP–Atb2 or mCherry–Atb2, the promoter region of *nda3*$^+$ gene and the coding sequences of GFP or mCherry and

Strains	Genotypes (w/ ura4-D18)
HR1316	lys1$^+$::P3nmt1–GFP–wee1 sid4$^+$::mRFP–kanR leu1-32 ade6-210 h$^-$
HR1477	wee1Δ::ura4$^+$ sid4$^+$::mRFP–kanR leu1-32 lys1-131 h$^-$
HR1518	lys1$^+$::P3nmt1–GFP–wee1-50 sid4$^+$::mRFP–kanR leu1-32 ade6-210 h$^-$
HR1606	kanR–GFP–wee1$^+$ sid4$^+$::mRFP–kanR leu1-32 h$^-$
HR1610	cdr2Δ::ura4$^+$ kanR–GFP–wee1$^+$ sid4$^+$::mRFP–kanR leu1-32 lys1-131 h$^-$
HR1689	wee1.V644::hphR aur1R–Pnda3–mCherry–atb2 sid4$^+$::mRFP–natR leu1-32 h$^-$
HR1752	pcp1-18::HA–hphR wee1.V644G::ura4$^+$ sid4$^+$::mRFP–natR aur1R–Pnda3–GFP–atb2 leu1-32 h$^-$
HR1924[(1)]	cdc13$^+$::GFP–LEU2 sid4$^+$::mRFP–kanR leu1-32 his2 ade6-216 h$^+$
HR2018	cdc13.117 kanR–GFP–wee1$^+$ sid4$^+$::mRFP–kanR h$^-$
HR2051	cdc13.117–GFP::natR h$^-$
HR2053	cdc13$^+$::GFP::natR sid4$^+$::mRFP–kanR leu1-32 lys1-131 h$^-$
Strains	**Genotypes (w/ leu1-32 ura4-D18 wee1Δ::ura4$^+$ h$^-$)**
HR1577	lys1$^+$::Pwee1–GFP–wee1 cut7$^+$::mCherry–kanR
HR1578	lys1$^+$::Pwee1–GFP–wee1 plo1$^+$::mCherry–hphR
HR1614	lys1$^+$::Pwee1–GFP–wee1 msd1$^+$::mCherry–hphR
HR1541	lys1$^+$::Pwee1–GFP–wee1 aur1$^+$::aur1R–Pnda3–mCherry–atb2
HR1917	pcp1$^+$::HA–hphR lys1$^+$::Pwee1–GFP–wee1
HR1943-1	pcp1$^+$::HA–hphR lys1$^+$::Pwee1–GFP–wee1.NLS1Δ2Δ
HR1961	pcp1$^+$::HA–hphR lys1$^+$::Pwee1–GFP–wee1.NES1Δ
HR1896-2	pcp1-18::HA–hphR lys1$^+$::Pwee1–GFP–wee1
HR1945-3	pcp1-18::HA–hphR lys1$^+$::Pwee1–GFP–wee1.NLS1Δ2Δ
HR1965	pcp1-18::HA–hphR lys1$^+$::Pwee1–GFP–wee1.NES1Δ
HR1911	cdr1Δ::kanR lys1$^+$::Pwee1–GFP–NESx2–wee1 sid4$^+$::mRFP–natR
HR1912	cdr1Δ::kanR lys1$^+$::Pwee1–GFP–wee1 sid4$^+$::mRFP–natR
HR1946	cdr1Δ::kanR lys1$^+$::Pwee1–GFP–wee1.NLS1Δ2Δ sid4$^+$::mRFP–natR
Strains	**Genotypes (w/ leu1-32 ura4-D18 wee1Δ::ura4$^+$ sid4$^+$::mRFP–kanR h$^-$)**
HR1481	lys1$^+$::Pwee1–GFP–wee1
HR1483	lys1$^+$::P81nmt1–GFP–wee1
HR1654	lys1$^+$::Pwee1–GFP–wee1.V644G
HR1658	lys1$^+$::Pwee1–GFP–wee1.V644G aur1R–Pnda3–GFP–atb2
HR1794	lys1$^+$::Pwee1–GFP–NESx2–wee1
HR1795	lys1$^+$::Pwee1–GFP–NLSx2–wee1
HR1928	lys1$^+$::Pwee1–GFP–wee1.NLS1Δ
HR1929	lys1$^+$::Pwee1–GFP–wee1.NLS1Δ2Δ
HR1939	lys1$^+$::Pwee1–GFP–wee1.NLS2Δ
HR1940	lys1$^+$::Pwee1–GFP–NLSx1–wee1
HR1803	lys1$^+$::Pwee1–GFP–Sid2N–wee1
HR1804	lys1$^+$::Pwee1–GFP–Sid4C–wee1
HR1942	lys1$^+$::Pwee1–GFP–wee1.NES1Δ
HR1967-1	lys1$^+$::Pwee1–GFP–CDx3–wee1
HR1971-1	lys1$^+$::Pwee1–GFP–BAF–wee1
HR1973-1	lys1$^+$::Pwee1–GFP–BAF.G47E–wee1
HR1505	cdr2Δ::ura4$^+$ lys1$^+$::Pwee1–GFP–wee1
HR2040	cdr2Δ::ura4$^+$ lys1$^+$::Pwee1–GFP–NESx2–wee1
HR2041	cdr2Δ::ura4$^+$ lys1$^+$::Pwee1–GFP–wee1.NLS1Δ2Δ
HR2009	lys1$^+$::Pwee1–3HA–wee1
HR2012	lys1$^+$::Pwee1–3HA–wee1.NLS1Δ2Δ
HR2013	lys1$^+$::Pwee1–3HA–wee1.NES1Δ
HR2015	lys1$^+$::Pwee1–3HA–wee1.NLS1Δ
HR2016	lys1$^+$::Pwee1–3HA–wee1.NLS2Δ
HR2020	lys1$^+$::Pwee1–3HA–NESx2–wee1.NLS1ΔNLS2Δ
HR2021	lys1$^+$::Pwee1–3HA–NESx2–wee1
HR2023	lys1$^+$::Pwee1–3HA–NLSx2–wee1
HR2024	lys1$^+$::Pwee1–3HA–NLSx1–wee1
HR2029	lys1$^+$::Pwee1–3HA–sid2N–wee1
HR2030	lys1$^+$::Pwee1–3HA–sid4C–wee1
HR2031	lys1$^+$::Pwee1–3HA–CD–wee1
HR2032	lys1$^+$::Pwee1–3HA–CDx2–wee1
HR2033	lys1$^+$::Pwee1–3HA–BAF–wee1
HR2034	lys1$^+$::Pwee1–3HA–BAF.G47E–wee1
HR2044	cut12.s11 lys1$^+$::Pwee1–GFP–wee1
HR2048	cut12.s11 lys1$^+$::Pwee1–GFP–NLSx2–wee1

TABLE 1: Strains used in this study. Reference: (1) Masuda *et al.* (2006a).

Atb2 were ligated at the *Sac*I/*Xho*I sites, at the *Xho*I/*Bam*HI sites, and at the *Bam*HI/*Apa*I sites, respectively, of pCST3 (Chikashige *et al.*, 2004; Masuda *et al.*, 2006b). The *lys1-N* fragment of the plasmid was replaced with *aur1R*, which is a selection marker for aureobasidin A (Chikashige *et al.*, 2004). The resulting plasmid was integrated at the *aur1* locus (Unsworth *et al.*, 2008).

Construction of 3HA-tagged Wee1 strains

To construct strains carrying 3HA–Wee1, 3HA–Wee1.NES1Δ, 3HA–Wee1.NLS1Δ, 3HA–Wee1.NLS2Δ, and 3HA–Wee1.NLS1Δ2Δ, the nmt1 promoter of pCST2 (Chikashige *et al.*, 2006) was replaced with the promoter region of *wee1*$^+$ at the *Pst*I/*Nde*I sites, and the entire coding region of the *wee1*$^+$ or *wee1* mutant genes was ligated in frame to the 3′ end of three copies of HA (3HA) at the *Xho*I/*Bgl*II sites. The resulting plasmids, pHRM1.3HA–Wee1 and other pHRM1.3HA–Wee1 mutant plasmids, were integrated into the chromosome at the *lys1* gene locus of cells with a *wee1* deletion background. To construct strains carrying 3HA–NLSx2–Wee1, 3HA–NLSx1–Wee1, 3HA–NESx2–Wee1, 3HA–NESx2–Wee1.NLS1Δ2Δ, 3HA–Sid2N–Wee1, 3HA–Sid4C–Wee1, 3HA–CD–Wee1, 3HA–CDx2–Wee1, 3HA–BAF–Wee1,

and 3HA–BAF.G47E–Wee1, the corresponding DNA fragments were inserted at *Xho*I sites of pHRM1.3HA–Wee1 or HRM1.3HA–Wee1.NLS1Δ2Δ, followed by integration of the resulting plasmids at the *lys1* locus of cells with a *wee1* deletion background.

Construction of *wee1.as1*

To construct a GFP–Wee1.as1 strain, a V644G mutation of Wee1 was introduced into the pHRM1GFP–Wee1 plasmid by site-directed mutagenesis. The resulting plasmid was integrated at the *lys1* locus in *wee1* deletion cells. The Wee1.as1 strain was constructed by replacing *wee1*$^+$ gene with *wee1.as1* using *hphR* as a selection marker by the PCR-based gene targeting method. 1-NM-PP1 (Calbiochem, La Jolla, CA) was used at 25 μM by dilution from a 10-mM stock dissolved in dimethyl sulfoxide.

Fluorescence microscopy

Fluorescence microscope images were obtained using the DeltaVision microscope system (Applied Precision, Seattle, WA) with a cooled CCD camera CoolSNAP.HQ (Photometrics, Tucson, AZ), which was set up in a temperature-controlled room as previously described (Haraguchi *et al.*, 1999) or equipped with a temperature-controlled chamber. Live cell imaging was performed at 36°C for temperature-sensitive mutants or at 26–27°C unless otherwise mentioned. Then 70 μl cells mixed with 130 μl EMM2 supplemented with amino acids were mounted in a glass-bottomed culture dish (MatTek, Ashland, MA) coated with soybean lectin (0.2 mg/ml).

Critical illumination with a mercury lamp was used for obtaining the images shown in Figures 1, 3A, and 6F with higher signal intensities. For quantification of Wee1 levels at the SPB, projection images of maximum intensity were obtained and maximum fluorescence intensities at the SPB were used for statistic data analysis. In some experiments, fluorescence intensity over the background intensity was used for statistic data analysis. For fixing cells for microscopy (Figure 7C), cells were incubated with 3.2% paraformaldehyde for 1 min, followed by incubation with paraformaldehyde and 0.3% glutaraldehyde for 9 min.

Preparation of denatured cell extracts, SDS–PAGE, and immunoblot analysis

Denatured cell extracts were prepared using the following method. First, 5–10 ml cells around 0.3 OD_{600} was incubated for 10 min with 1 mM phenylmethylsulfonyl fluoride (PMSF), collected, and resuspended in 800 μl ice-cold water with 1 mM PMSF. The cell suspensions were mixed with 150 μl 1.85 N NaOH and incubated for 10 min on ice. Then 150 μl of 55% (wt/vol) trichloroacetic acid was added, and the mixture was incubated for 10 min on ice. The cells were pelleted at 5000 rpm for 5 min at 4°C, resuspended in 100 μl HU buffer (8M urea, 5% SDS, 200 mM NaPO4 [pH 6.8], 0.1 mM EDTA, 100 mM dithiothreitol, and bromophenol blue) per OD_{600} of cells, and incubated at 65°C for 10 min. Then 10 μl denatured cell extracts were loaded onto NuPAGE 4–12% Bis-Tris gels (Invitrogen, San Diego, CA). The proteins separated by SDS–PAGE were transferred onto the polyvinylidene difluoride membrane. After it was blocked with 5% skim milk in phosphate-buffered saline, the membrane was first incubated with anti-HA (12CA5) (Roche, Basel, Switzerland) or anti–α-tubulin (B-5-1-2) (Sigma-Aldrich, St. Louis, MO) and then with horseradish peroxidase–conjugated anti–mouse immunoglobulin G. Detection and quantification of 3HA–Wee1 and 3HA–Wee1 mutant proteins were performed with enhanced chemiluminescence reagents using BioRad ChemiDoc XRS Plus and the Image Lab software.

ACKNOWLEDGMENTS

We thank Takashi Toda at Cancer Research UK for discussion and advice and for allowing work to be carried out in his laboratory. We thank Iain Hagan, Jacky Hayles, Jamie Moseley, and Paul Russell for strains. This work is partly supported by Kakenhi from the Ministry of Education, Culture, Sports, Science, and Technology (to T. H. and Y. H.) and by Cancer Research UK.

REFERENCES

Alfa CE, Ducommun B, Beach D, Hyams JS (1990). Distinct nuclear and spindle pole body populations of cyclin–cdc2 in fission yeast. Nature 347, 680–682.

Bähler J, Wu JQ, Longtine MS, Shah NG, McKenzie A III, Steever AB, Wach A, Philippsen P, Pringle JR (1998). Heterologous modules for efficient and versatile PCR-based gene targeting in *Schizosaccharomyces pombe*. Yeast 14, 943–951.

Baldin V, Ducommun B (1995). Subcellular localisation of human wee1 kinase is regulated during the cell cycle. J Cell Sci 108, 2425–2432.

Bishop AC *et al.* (2000). A chemical switch for inhibitor-sensitive alleles of any protein kinase. Nature 407, 395–401.

Booher RN, Alfa CE, Hyams JS, Beach DH (1989). The fission yeast cdc2/cdc13/suc1 protein kinase: regulation of catalytic activity and nuclear localization. Cell 58, 485–497.

Chikashige Y, Kurokawa R, Haraguchi T, Hiraoka Y (2004). Meiosis induced by inactivation of Pat1 kinase proceeds with aberrant nuclear positioning of centromeres in the fission yeast *Schizosaccharomyces pombe*. Genes Cells 9, 671–684.

Chikashige Y, Tsutsumi C, Yamane M, Okamasa K, Haraguchi T, Hiraoka Y (2006). Meiotic proteins Bqt1 and Bqt2 tether telomeres to form the bouquet arrangement of chromosomes. Cell 125, 59–69.

Chang L, Gould KL (2000). Sid4p is required to localize components of the septation initiation pathway to the spindle pole body in fission yeast. Proc Natl Acad Sci USA 97, 5249–5254.

Chin CF, Yeong FM (2010). Safeguarding entry into mitosis: the antephase checkpoint. Mol Cell Biol 30, 22–32.

Dalal SN, Schweitzer CM, Gan J, DeCaprio JA (1999). Cytoplasmic localization of human cdc25C during interphase requires an intact 14-3-3 binding site. Mol Cell Biol 19, 4465–4479.

Decottignies A, Zarzov P, Nurse P (2001). In vivo localisation of fission yeast cyclin-dependent kinase cdc2p and cyclin B cdc13p during mitosis and meiosis. J Cell Sci 114, 2627–2640.

Deibler RW, Kirschner MW (2010). Quantitative reconstitution of mitotic CDK1 activation in somatic cell extracts. Mol Cell 37, 753–767.

Ding D-Q, Tomita Y, Yamamoto A, Chikashige Y, Haraguchi T, Hiraoka Y (2000). Large-scale screening of intracellular protein localization in living fission yeast cells by the use of a GFP-fusion genomic DNA library. Genes Cells 5, 169–190.

Ding R, West RR, Morphew DM, Oakley BR, McIntosh JR (1997). The spindle pole body of *Schizosaccharomyces pombe* enters and leaves the nuclear envelope as the cell cycle proceeds. Mol Biol Cell 8, 1461–1479.

Doxsey S, McCollum D, Theurkauf W (2005). Centrosomes in cellular regulation. Annu Rev Cell Dev Biol 21, 411–434.

Flory MR, Morphew M, Joseph JD, Means AR, Davis TN (2002). Pcp1p, an Spc110p-related calmodulin target at the centrosome of the fission yeast *Schizosaccharomyces pombe*. Cell Growth Differ 13, 47–58.

Fong CS, Sato M, Toda T (2009). Fission yeast Pcp1 links polo kinase-mediated mitotic entry to γ-tubulin-dependent spindle formation. EMBO J 29, 120–130.

Funabiki H, Hagan I, Uzawa S, Yanagida M (1993). Cell cycle-dependent specific positioning and clustering of centromeres and telomeres in fission yeast. J Cell Biol 121, 961–976.

Gavet O, Pines J (2010). Progressive activation of CyclinB1-Cdk1 coordinates entry to mitosis. Dev Cell 18, 533–543.

Hagan IM (2008). The spindle pole body plays a key role in controlling mitotic commitment in the fission yeast *Schizosaccharomyces pombe*. Biochem Soc Trans 36, 1097–1101.

Hagan I, Yanagida M (1992). Kinesin-related cut7 protein associates with mitotic and meiotic spindles in fission yeast. Nature 347, 563–566.

Hagting A, Karlsson C, Clute P, Jackman M, Pines J (1998). MPF localization is controlled by nuclear export. EMBO J 17, 4127–4138.

Haraguchi T, Ding D-Q, Yamamoto A, Kaneda T, Koujin T, Hiraoka Y (1999). Multiple-color fluorescence imaging of chromosomes and microtubules in living cells. Cell Struct Funct 24, 291–298.

Haraguchi T, Kojidani T, Koujin T, Shimi T, Osakada H, Mori C, Yamamoto A, Hiraoka Y (2008). Live cell imaging and electron microscopy reveal dynamic processes of BAF-directed nuclear envelope assembly. J Cell Sci 121, 2540–2554.

Heald R, McLoughlin M, McKeon F (1993). Human wee1 maintains mitotic timing by protecting the nucleus from cytoplasmically activated Cdc2 kinase. Cell 74, 463–474.

Jackman M, Lindon C, Nigg EA, Pines J (2003). Active cyclin B1-Cdk1 first appears on centrosomes in prophase. Nat Cell Biol 5, 143–148.

Jin P, Hardy S, Morgan DO (1998). Nuclear localization of cyclin B1 controls mitotic entry after DNA damage. J Cell Biol 141, 875–885.

Kitajima TS, Sakuno T, Ishiguro K, Iemura S, Natsume T, Kawashima SA, Watanabe Y (2006). Shugoshin collaborates with protein phosphatase 2A to protect cohesin. Nature 441, 46–52.

Krapp A, Simanis V (2008). An overview of the fission yeast septation initiation network (SIN). Biochem Soc Trans 36, 411–415.

Kumagai A, Dunphy WG (1999). Binding of 14-3-3 proteins and nuclear export control the intracellular localization of the mitotic inducer Cdc25. Genes Dev 13, 1067–1072.

Kunz D, Luley C, Winkler K, Lins H, Kunz WS (1997). Flow cytometric detection of mitochondrial dysfunction in subpopulations of human mononuclear cells. Anal Biochem 246, 218–224.

Lee MS, Craigie R (1998). A previously unidentified host protein protects retroviral DNA from autointegration. Proc Natl Acad Sci USA 95, 1528–1533.

Lindqvist A, Källström H, Lundgren A, Barsoum E, Rosenthal CK (2005). Cdc25B cooperates with Cdc25A to induce mitosis but has a unique role in activating cyclin B1-Cdk1 at the centrosome. J Cell Biol 171, 35–45.

Lindqvist A, van Zon W, Rosenthal CK, Wolthuis RMF (2007). Cyclin B1–Cdk1 activation continues after centrosome separation to control mitotic progression. PLoS Biology 5, 1128–1137.

Lopez-Girona A, Furnari B, Mondesert O, Russell P (1999). Nuclear localization of Cdc25 is regulated by DNA damage and a 14-3-3 protein. Nature 397, 172–175.

MacIver FH, Tanaka K, Robertson AM, Hagan IM (2003). Physical and functional interactions between Polo kinase and the spindle pole component Cut12 regulate mitotic commitment in *S. pombe*. Genes Dev 17, 1507–1523.

Martin SG, Berthelot-Grosjean M (2009). Polar gradients of the DYRK-family kinase Pom1 couple cell length with the cell cycle. Nature 459, 852–856.

Masuda H, Toda T, Miyamoto R, Haraguchi T, Hiraoka Y (2006a). Modulation of Alp4 function in *Schizosaccharomyces pombe* induces novel phenotypes that imply distinct functions for the nuclear and cytoplasmic-γ-tubulin complexes. Genes Cells 11, 319–336.

Masuda H, Miyamoto R, Haraguchi T, Hiraoka Y (2006b). The carboxy-terminus of Alp4 alters microtubule dynamics to induce oscillatory nuclear movement led by the spindle pole body in *Schizosaccharomyces pombe*. Genes Cells 11, 337–352.

Matsuyama A *et al*. (2006). ORFeome cloning and global analysis of protein localization in the fission yeast *Schizosaccharomyces pombe*. Nat Biotechnol 24, 841–847.

Matsusaka T, Pines J (2004). Chfr acts with the p38 stress kinases to block entry to mitosis in mammalian cells. J Cell Biol 166, 507–516.

McGowan CH, Russell P (1995). Cell cycle regulation of human WEE1. EMBO J 14, 2166–2175.

Moreno S, Klar A, Nurse P (1991). Molecular analysis of the fission yeast *Schizosaccharomyces pombe*. Methods Enzymol 194, 795– 823.

Morrell JL *et al*. (2004). Sid4p-Cdc11p assembles the septation initiation network and its regulators at the *S. pombe* SPB. Curr Biol 14, 579–584.

Moseley JB, Mayeux A, Paoletti A, Nurse P (2009). A spatial gradient coordinates cell size and mitotic entry in fission yeast. Nature 459, 857–860.

Mulvihill DP, Petersen J, Ohkura H, Glover DM, Hagan IM (1999). Plo1 kinase recruitment to the spindle pole body and its role in cell division in *Schizosaccharomyces pombe*. Mol Biol Cell 10, 2771–2785.

Nurse P (1990). Universal control mechanism regulating onset of M-phase. Nature 344, 503–508.

Oh JS, Han SJ, Conti M (2010). Wee1B, Myt1, and Cdc25 function in distinct compartments of the mouse oocyte to control meiotic resumption. J Cell Biol 188, 199–207.

Parker LL, Atherton-Fessler S, Piwnica-Worms H (1992). p107wee1 is a dual-specificity kinase that phosphorylates p34cdc2 on tyrosine 15. Proc Natl Acad Sci USA 89, 2917–2921.

Petersen J, Hagan IM (2005). Polo kinase links the stress pathway to cell cycle control and tip growth in fission yeast. Nature 435, 507–512.

Segura-Totten M, Kowalski AK, Craigie R, Wilson KL (2002). Barrier-to-autointegration factor: major roles in chromatin decondensation and nuclear assembly. J Cell Biol 158, 475–485.

Sparks CA, Morphew M, McCollum D (1999). Sid2p, a spindle pole body kinase that regulates the onset of cytokinesis. J Cell Biol 146, 777–790.

Tallada VA, Tanaka K, Yanagida M, Hagan IM (2009). The *S. pombe* mitotic regulator Cut12 promotes spindle pole body activation and integration into the nuclear envelope. J Cell Biol 185, 875–888.

Tomlin GC, Morrell JL, Gould KL (2002). The spindle pole body protein Cdc11p links Sid4p to the fission yeast septation initiation network. Mol Biol Cell 13, 1203–1214.

Toya M, Sato M, Haselmann U, Asakawa K, Brunner D, Antony C, Toda T (2007). γ-Tubulin complex-mediated anchoring of spindle microtubules to spindle-pole bodies requires Msd1 in fission yeast. Nat Cell Biol 9, 646–653.

Toyoshima F, Moriguchi T, Wada A, Fukuda M, Nishida E (1998). Nuclear export of cyclin B1 and its possible role in the DNA damage-induced G_2 checkpoint. EMBO J 17, 2728–2735.

Unsworth A, Masuda H, Dhut S, Toda T (2008). Fission yeast kinesin-8 Klp5 and Klp6 are interdependent for mitotic nuclear retention and required for proper microtubule dynamics. Mol Biol Cell 19, 5104–5115.

Wu L, Shiozaki K, Aligue R, Russell P (1996). Spatial organization of the Nim1-Wee1-Cdc2 mitotic control network in *Schizosaccharomyces pombe*. Mol Biol Cell 7, 1749–1758.

Yanagida M, Yamashita YM, Tatebe H, Ishii K, Kumada K, Nakaseko Y (1999). Control of metaphase-anaphase progression by proteolysis: cyclosome function regulated by the protein kinase A pathway, ubiquitination and localization. Phil Trans R Soc Lond B 354, 1559–1570.

Yang J, Bardes ES, Moore JD, Brennan J, Powers MA, Kornbluth S (1998). Control of cyclin B1 localization through regulated binding of the nuclear export factor CRM1. Genes Dev 12, 2131–2143.